

## Article

# Restoring Functional Soil Depth in Plinthosols: Effects of Subsoiling and Termite Mound Amendments on Maize Yield

John Banza Mukalay <sup>1,2,\*</sup>, Jeroen Meersmans <sup>1</sup>, Joost Wellens <sup>1,3</sup>, Yannick Useni Sikuzani <sup>4</sup>, Emery Kasongo Lenge Mukonzo <sup>5</sup> and Gilles Colinet <sup>1,\*</sup>

<sup>1</sup> Water-Soil-Plant Exchange Research Unit, TERRA Gembloux Agro-Bio-Tech, University of Liège, 5030 Gembloux, Belgium; jeroen.meersmans@uliege.be (J.M.); joost.wellens@uliege.be (J.W.)

<sup>2</sup> Department of Renewable Natural Resource Management, Faculty of Agricultural Sciences and Environment, University of Kolwezi, Kolwezi P.O. Box 57, Democratic Republic of the Congo

<sup>3</sup> Environmental Sciences and Management Department, University of Liège, Avenue de Longwy 185, 6700 Arlon, Belgium

<sup>4</sup> Ecologie, Restauration Écologique et Paysage, Faculté des Sciences Agronomiques, University of Lubumbashi, Lubumbashi P.O. Box 1825, Democratic Republic of the Congo; sikuzaniu@unilu.ac.cd

<sup>5</sup> Land Assessment, Soil Conservation and Agro-Meteorology Research Unit, Faculty of Agronomy, University of Lubumbashi, Lubumbashi P.O. Box 1825, Democratic Republic of the Congo; kasongolenge@gmail.com

\* Correspondence: john.banzamukalay@uliege.be or mukalayjohn@gmail.com (J.B.M.); gilles.colinet@uliege.be (G.C.)

## Abstract

Soil degradation and limited root-exploitable depth restrict maize productivity in Plinthosols of tropical regions. However, the combined effects of subsoiling and amendments derived from termite mound materials on soil functionality and yield remain insufficiently quantified. This study examines how variations in a functionally exploitable rooting depth, within a management system combining subsoiling and termite mound amendments, are associated with soil physicochemical properties and spatial variability of maize (*Zea mays* L.) grain yield in the Lubumbashi region of the Democratic Republic of the Congo. Spatial soil sampling and correlation analyses were used to identify the dominant pedological factors controlling yield variability. The results indicate a reduced vertical stratification of most nutrients within the explored depth, reflecting a more homogeneous distribution of soil properties within the managed profile, although direct causal attribution to specific practices cannot be established in the absence of untreated control plots. Improved rooting conditions were reflected by high and spatially variable productivity (2.3 to 11.1 t ha<sup>-1</sup> across blocks), accompanied by a moderate average gain between seasons (<1 t ha<sup>-1</sup>), while extractable manganese emerged as a consistent negative predictor of yield. These patterns are consistent with a larger functionally exploitable rooting depth and an improved soil environment, although causal contributions of subsoiling and termite mound amendments cannot be isolated in the absence of control plots. Overall, the results highlight the importance of jointly considering structural and chemical soil properties when interpreting productivity gradients in Plinthosols and designing sustainable management strategies for degraded tropical soils.

**Keywords:** Plinthosols; maize (*Zea mays* L.); spline with barriers; subsoiling; termite mound materials; Lubumbashi



Academic Editor: Joaquim Esteves Da Silva

Received: 16 December 2025

Revised: 7 January 2026

Accepted: 15 January 2026

Published: 17 January 2026

**Copyright:** © 2026 by the authors.

Licensee MDPI, Basel, Switzerland.

This article is an open access article distributed under the terms and

conditions of the [Creative Commons](https://creativecommons.org/licenses/by/4.0/)

[Attribution \(CC BY\)](https://creativecommons.org/licenses/by/4.0/) license.

## 1. Introduction

Agricultural productivity in tropical regions is closely dependent on the physicochemical quality of soils, which controls water availability, nutrient availability, and plant rooting conditions [1–4]. In the Lubumbashi region, in the southeast of the Democratic Republic of the Congo, the dominant soils are ferralitic soils with low intrinsic fertility and the occurrence of plinthite, characterized by a compact structure, low organic matter content, and high acidity, limiting the availability of essential nutrients [5–7]. The frequent presence of plinthite at shallow depths exacerbates these constraints, hindering root growth and limiting the productivity of maize (*Zea mays* L.), the main food crop and basis of regional food security [8–11].

Faced with these limitations, innovative soil management approaches have been tested to restore fertility and improve the structure of Plinthosols. Among these, amendments with giant termite mound materials and mechanical subsoiling appear to be two promising practices capable of correcting the physical and chemical constraints that limit agricultural production [12–14]. Termite mound materials, rich in clay and basic cations ( $\text{Ca}^{2+}$ ,  $\text{Mg}^{2+}$ ,  $\text{K}^+$ ), contribute to acidity neutralization and improved cation exchange capacity [15–18]. At the same time, subsoiling breaks up hardened horizons, improves porosity, macropore continuity, and drainage, thereby promoting deeper and more uniform root penetration [19–25].

Subsoiling and amendments derived from termite mound materials have been reported to improve rooting conditions and nutrient distribution in compacted tropical soils, although their effects may vary depending on soil type, depth, and management history [13,26]. The combined action of these two practices results in improved water and nutrient availability, promoting more vigorous vegetative growth and increased yields, particularly for maize, a crop that is highly dependent on a large volume of exploitable soil and a functional root system [27–31]. However, in Plinthosols, the effectiveness of these practices is closely linked to the depth actually accessible to roots, which is strongly controlled by the position and thickness of the plinthite [32].

To date, studies conducted in the Lubumbashi region have mainly focused on the effect of termite mound materials applied to the surface, without explicitly integrating the role of subsoiling or the spatial variability of the usable depth related to the plinthitic crust [13,33,34]. This gap limits our understanding of how the root zone actually functions in these challenging soils and highlights the need for an integrated approach, combining chemical improvement and physical restructuring of the profile.

Recent studies in compacted tropical and subtropical soils have shown that deep tillage and subsoiling can reduce bulk density in the 20–40 cm layer, improve porosity and rooting depth, and increase maize yield by 10–30% under field conditions [35–38]. In parallel, termite mound materials are increasingly recognized as biogenic amendments that enrich soils with fine clays, base cations, and organo-mineral complexes, improving cation exchange capacity, water retention, and microbial functioning [15,39–44]. However, these approaches have largely been evaluated separately and rarely within Plinthosols, where plinthite strongly constrains rooting depth. To our knowledge, no study has examined how restoring a functionally exploitable depth in Plinthosols through the combined effects of subsoiling and termite mound amendments reshapes soil functioning and controls spatial variability in maize yield. This gap motivates the present study.

In this context, the 0–40 cm depth was selected as the zone that is effectively made physically and chemically exploitable in this Plinthosol following deep mechanical intervention. Although this interval does not correspond to a single homogeneous pedogenetic horizon, it represents a functionally relevant depth that delimits the volume of soil actually accessible to maize roots once compaction is reduced. This choice is consistent with previous studies showing that, when mechanical constraints are alleviated, maize can

effectively explore soil volumes down to approximately 40 cm or more, thereby benefiting from increased access to water and nutrients [44–46]. The surface horizon (0–10 cm), which has a more constant thickness and is strongly influenced by cultivation practices [47], was analyzed in parallel as a comparative reference. However, its results are presented separately in the Supplementary Materials, as the central objective of this study is to interpret soil–yield relationships within the mechanically loosened rooting zone where functional changes are most pronounced.

This study has the principal objective of determining how restoring a functionally exploitable rooting depth through subsoiling combined with amendments from termite mound materials modifies the physicochemical properties of Plinthosols and explains the spatial variability of maize grain yield in the Lubumbashi region. The central hypothesis is that alleviating mechanical constraints, together with chemical enrichment of the soil, enhances the functional root zone and leads to a measurable increase in maize productivity. More specifically, this study seeks to (1) characterize the spatial variability of soil physicochemical properties within the functionally restored 0–40 cm layer; (2) identify the dominant pedological factors structuring edaphic variability under conditions of improved exploitable depth; (3) quantify the relative contribution of these properties to maize yield variability across blocks; and (4) determine the most decisive soil factors for productivity in order to optimize the integrated management of Plinthosols in tropical agricultural systems. These objectives translate into the following research questions: (i) To what extent does restoring a functionally exploitable depth improve maize yield in Plinthosols? (ii) Which soil physicochemical properties best predict yield variability once mechanical constraints are alleviated? (iii) Do structural and chemical improvements interact over time to enhance maize productivity?

## 2. Materials and Methods

### 2.1. Study Sites

The study was conducted on the FarmCo agricultural site, located in the Lubumbashi region, Haut-Katanga province, Democratic Republic of the Congo. The study area is located approximately 60 km east of Lubumbashi, along the national road leading to Kasenga, in the Kifumanshi River valley (Figure 1). The study area is located at an elevation of approximately 1245–1300 m a.s.l. on gently undulating geomorphological surfaces (<5% slope), underlain by schists and quartzites of the Katangan Supergroup [5].

This estate, with a total area of 660 ha, is one of the largest farms in the region, known for its industrial production of maize grain for local processing into flour for consumption. Its soil cover is mainly characterized by Plinthosols sensu FAO, corresponding to plinthic ferralsols according to the WRB [48] classification. These soils are characterized by shallow depth, high compaction of the lower horizons, and, in the case of the Ferralsols, marked textural variability, limiting their suitability for cultivation without mechanical intervention or appropriate amendments. In order to improve productivity, the site underwent excavation of the lateritic benches, combined with deep subsoiling around the entire perimeter. Subsoiling was carried out using a tree-shank ripper operating at a target depth of  $\geq 40$  cm, breaking up plinthite continuity and increasing the volume of soil effectively usable by the root system.

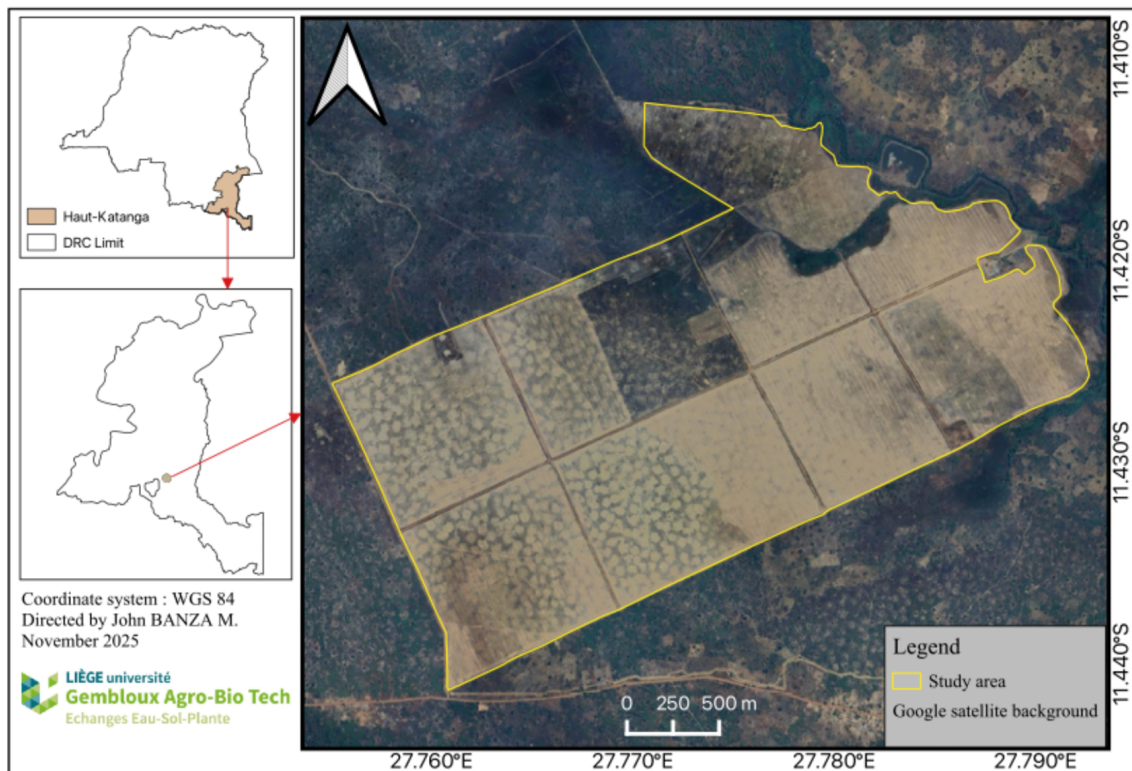


**Figure 1.** Location of the study site, FarmCo farm in Lubumbashi in the province of Haut-Katanga.

At the same time, materials from giant termite mounds, which are abundant on the site, were excavated and spread more or less evenly. This operation aimed to level the ground and make use of these materials as soil amendments, thanks to their richness in clay and basic cations (Figure 2). In this region, the average density of inactive constructed by *Macrotermes falciger* termite mounds is estimated at around seven structures per hectare, each with an average individual volume of around 256 m<sup>3</sup> [12]. The total theoretically mobilizable volume thus reaches nearly 1800 m<sup>3</sup> ha<sup>-1</sup>.



**Figure 2.** (A): Plinthite blocks extracted and deposited off-site after subsoiling; (B): excavation of a termite mound used as a source of soil amendment material; (C): Maize field in full growth after subsoiling and amendment with termite mound material (photo credit John Banza M.).

Considering a uniform distribution of this material on the soil surface, this would correspond to an average thickness of approximately  $18 \pm 2.3 \text{ cm ha}^{-1}$ , or the equivalent of approximately  $2000 \text{ t ha}^{-1}$ , based on an estimated bulk density of  $1.2 \text{ g cm}^{-3}$  [16]. Although all experimental blocks received termite mound material, a larger amount was applied in areas where plinthite had been more extensively excavated, to ensure uniform leveling of the plot and to compensate for the volume of soil lost during subsoiling operations.

From a climatic point of view, the region has a humid subtropical climate with dry winters (type  $C_{W6}$ ) according to the Köppen classification [49]. The rainfall pattern consists of a rainy season from November to March, a dry season from May to September, and two transition months (April and October). Average annual rainfall is estimated at 1270 mm, while the average annual temperature is 20.1 °C, with extremes ranging from 8 °C in the cold season to 32 °C in the hot season [50]. Figure 3 below illustrates the meteorological dynamics observed during the 2022–2023 and 2023–2024 growing seasons. The variables analyzed show similar trends between the two seasons. The meteorological data series used comes from the NASA POWER satellite database (CERES/MERRA-2; <https://power.larc.nasa.gov/data-access-viewer/>, accessed on 10 February 2025). This source was chosen due to the absence of operational and continuously functioning weather stations in the study area, thus ensuring complete and consistent temporal coverage for the entire period under consideration.

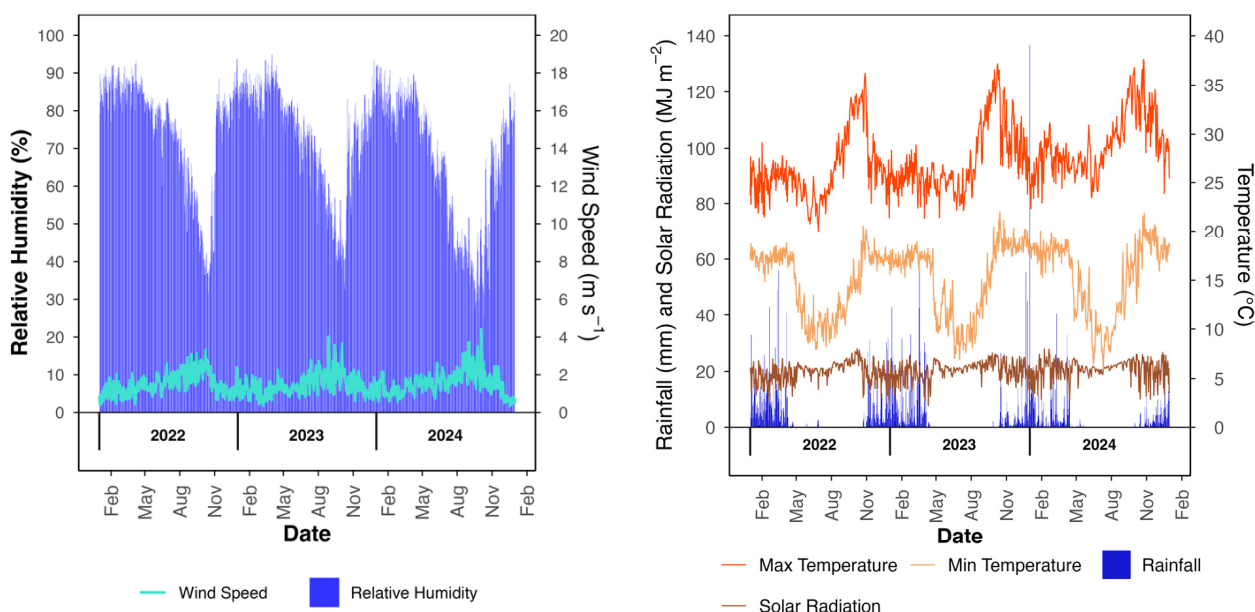


**Figure 3.** Meteorological characteristics recorded at the study site during the 2022–2023 and 2023–2024 growing seasons.

## 2.2. Sampling and Laboratory Analysis

Spatial sampling was carried out across the entire study area, covering approximately 660 ha, subdivided into ten experimental blocks (B1 to B10). In each block, five sampling points were positioned to ensure good spatial representativeness, with one point located approximately at the center of the block and four additional points distributed toward the corners, while maintaining a minimum distance of 200 m from the block boundaries to avoid edge effects (Figure 4). This approach corresponds to spatially structured sampling, designed to capture intra-block heterogeneity, rather than strictly random computer-generated sampling.

Samples were taken using a soil auger at two depths: 0–10 cm and 0–40 cm. The 0–10 cm layer corresponds to the surface horizon, which is directly influenced by farming practices and is of relatively constant thickness across the entire site. The 0–40 cm depth corresponds to the area that has been made physically and chemically exploitable in this Plinthosol by subsoiling, as the subsoiler was used at a depth of at least 40 cm. It is therefore an appropriate functional depth for assessing the combined impact of subsoiling and amendment with termite mound material.

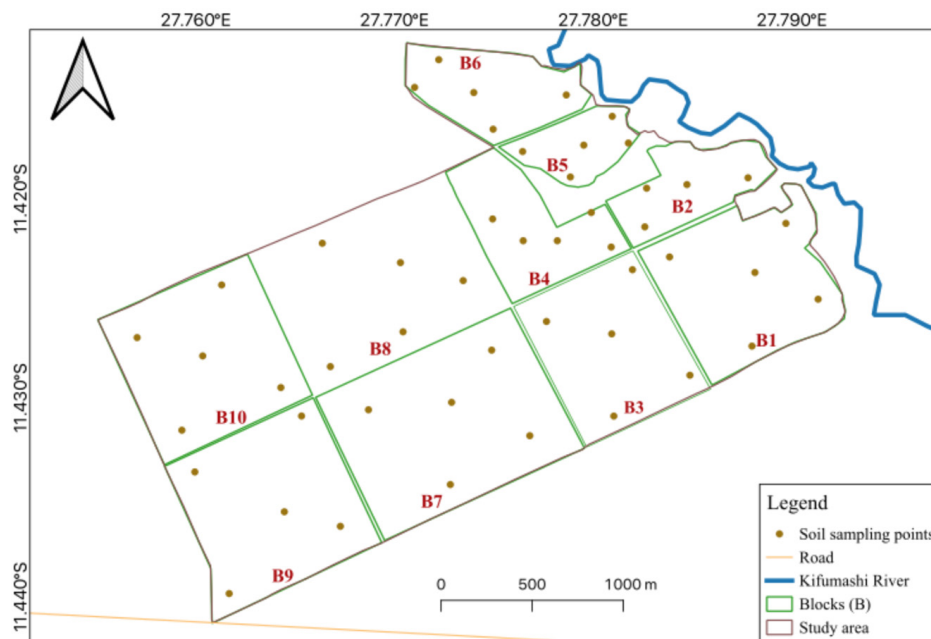


**Figure 4.** Soil sampling plan for the site showing the ten experimental blocks (B1–B10) and the spatial distribution of sampling points within each block.

Although the subsoiler occasionally reached depths greater than 40 cm in blocks where plinthite was less resistant, the 40 cm depth represents the minimum threshold at which mechanical constraints were consistently alleviated across all sampling units. Above this depth, rooting conditions were effectively restored and nutrient redistribution occurred, whereas below it the plinthite layer remained limiting. Consequently, 40 cm provides a standardized analytical depth corresponding to the volume of soil that was reliably rendered exploitable for maize roots throughout the study area. A conceptual schematic illustrating this restored exploitable rooting depth and its relation to plinthite is presented in Figure 5.

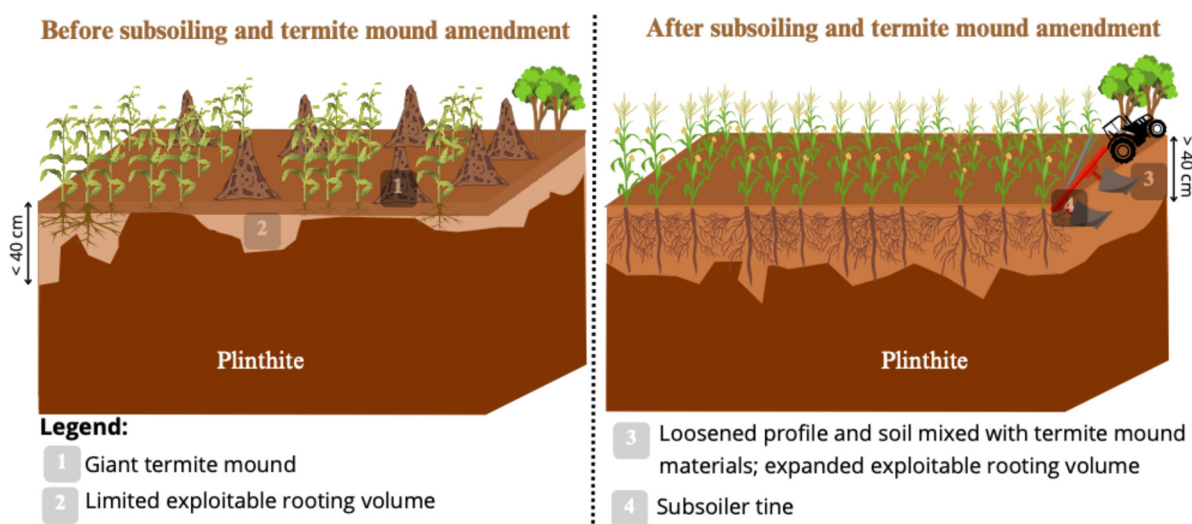


**Figure 5.** Conceptual diagram illustrating changes in root-accessible volume before and after integrated subsoiling and amendment with termite mound materials in Plinthosols of the Lubumbashi region.

In this study, the main analysis focused on the depth of 0–40 cm, considered to be the active root zone of the soil after intervention. The results for the 0–10 cm layer are presented in the Supplementary Materials to support the interpretation of the processes

of vertical redistribution and profile mixing. A total of 100 disturbed soil samples were collected (50 for each depth). The samples were air-dried for five days, sieved to 2 mm, and then conditioned for laboratory analysis.

Soil analyses were carried out at the soil chemistry laboratory of Gembloux Agro-Bio-Tech, Belgium. Soil pH was measured in water and in 1 N KCl following Van Reeuwijk [51]. Total organic carbon (TOC) was determined using the Walkley and Black wet oxidation method [52], with a correction factor of 1.33 applied to account for incomplete oxidation. Soil organic matter (SOM) was estimated from TOC using a conversion factor of 2, as recommended by Pribyl [53].

Available macronutrients (Ca, Mg, K, P) and trace elements (Cu, Fe, Al, Mn) were extracted using the ammonium acetate–EDTA method at pH 4.65 according to Houba et al. [54]. Phosphorus was quantified colorimetrically, while cations and trace metals were measured using inductively coupled plasma optical emission spectrometry (ICP-OES). All analytical procedures followed internationally recognized standards and are well suited to ferrallitic and plinthic tropical soils, where ferric and aluminous phases require complexing extractants to ensure reliable quantification.

### 2.3. Yield Determination

The grain maize yield was measured in a 1 m<sup>2</sup> plot repeated at least five times in each block, following the formula of Tandzi & Mutengwa [55] (Yield; Equation (1)). This method is widely used in agricultural operations because it allows for a quick and accurate estimation of yields [56]. During the first growing season (2022–2023), 41 observation plots were marked out across the entire site. The geographical coordinates of each plot were recorded using a Garmin 66R GPS (accuracy < 1 m), which made it possible to relocate and sample the same 41 locations during the second season (2023–2024), thereby ensuring full spatial comparability of yield measurements between seasons.

$$\text{Yield (kg ha}^{-1}\text{)} = \left[ \left( \text{number of rows of grain per ear} \times \frac{\text{number of ears per m}^2}{100} \right) \times \left( \text{Weight of 1000} - \frac{\text{grains (g)}}{10,000} \right) \times 10,000 \right] \quad (1)$$

During both growing seasons, maize (variety SC719) was cultivated over a full production cycle of approximately 210–215 days (late November to late June), based on sowing dates ranging from 22 November to 2 December and harvest dates from 22 to 30 June across blocks. The crop was sown at a spacing of 0.75 m × 0.25 m, corresponding to a density of 53,333 plants ha<sup>-1</sup>. Cultivation practices were uniform across all blocks: mechanical soil preparation (plowing + harrowing), sowing, mineral fertilization, and pre-emergence herbicide application. A basic NPK fertilizer (10-20-10) was applied at sowing at a rate of 200 kg ha<sup>-1</sup>, followed by urea 45 days after sowing (200 kg ha<sup>-1</sup>).

Between the two growing seasons, all blocks were managed uniformly. After harvest, crop residues were left on the soil surface until the onset of field operations for the following season. Prior to sowing, residues were incorporated by plowing followed by harrowing, and no additional amendments or mechanical deep tillage were applied beyond the initial subsoiling operation. The soil surface remained bare during the dry season due to the absence of cover crops, which is standard practice in the region and reflects operational conditions on the site. This uniform management ensured that seasonal differences in yield could not be attributed to contrasting inter-season soil treatments.

### 2.4. Spatial Analysis of Yield

In order to characterize the spatial variability of grain maize yield at the scale of the study area, a geostatistical analysis was performed using ArcGIS 10.8.1. Several interpolation methods were tested [57]. Four main classes of interpolation approaches were considered. Kriging is a geostatistical method that predicts unsampled values using variogram-derived spatial autocorrelation. Inverse Distance Weighting (IDW) is a deterministic method in which estimated values are calculated as a distance-weighted average of nearby observations, giving more influence to closer points. Spline interpolation fits a smooth surface through measured points by minimizing curvature, while its

“Spline With Barriers” variant constrains surface fitting to respect spatial discontinuities such as block boundaries. In this study, “barriers” correspond to block boundaries digitized as spatial discontinuities. These boundaries constrain interpolation to respect historical and operational differences between blocks, preventing artificial smoothing across management units and preserving the spatial structure of yield variability. Natural Neighbor interpolation estimates values based on the proportionate area shared between Voronoi polygons of sampled and prediction locations, producing smooth transitions while avoiding overshooting and preserving local gradients [57]. Kriging was explored based on the analysis of semivariograms, but no clear spatial dependency structure could be identified, justifying its exclusion (Figures S1 and S2). The Inverse Distance Weighted (IDW) and Spline were also evaluated, but generated significant visual artifacts, including “bull’s eye” effects, reflecting unrealistic interpolation. Conversely, the Natural Neighbor and Spline With Barriers methods produced visually consistent interpolated surfaces that were better suited to the distribution of points.

To decide between the two models, automated cross-validation was performed in ModelBuilder, running 100 simulation iterations. At each iteration, 90% of the data was used for model calibration and the remaining 10% for validation, using a random resampling procedure. Predictive performance was evaluated using two complementary statistical indicators: (i) root mean square error (RMSE), which quantifies the average difference between observed and predicted values, with low values (ideally  $<1 \text{ t ha}^{-1}$  for yield) indicating better model accuracy [58]; and (ii) bias, which measures the model’s tendency to overestimate or underestimate the variable of interest, with a value close to zero indicating the absence of systematic bias and greater reliability of predictions [59]. The two metrics were calculated according to (RMSE; Equation (2)) and (Bias; Equation (3)):

$$RMSE = \sqrt{\frac{1}{n} \sum_{i=1}^n (P_{obs(i)} - P_{pred(i)})^2} \quad (2)$$

$$Bias = \frac{1}{n} \sum_{i=1}^n (P_{obs(i)} - P_{pred(i)}) \quad (3)$$

where  $n$  is the total number of samples used in the validation procedure,  $P_{obs(i)}$  is the value of the  $i$ -th observation in the validation dataset, and  $P_{pred(i)}$  is the predicted value for the  $i$ -th observation.

The cross-validation results indicate that the Spline With Barriers method has the lowest RMSE values and a bias close to zero. This reflects greater prediction accuracy and a reduction in interpolation artifacts, particularly in areas where the spatial continuity of the phenomenon is constrained. As a result, Spline With Barriers was selected as the optimal method for interpolating observed yields and generating the spatial maps used in this study (Figure S3). After spatial interpolation of yields and generation of the associated maps, the soil sampling points were superimposed on the interpolated surfaces. This superimposition made it possible to extract, for each georeferenced point, the estimated yield value at the corresponding pixel. The measured soil data were then matched to the interpolated yields, ensuring a consistent spatial coupling between soil properties and observed production. This soil-yield matching served as the basis for subsequent statistical analyses, including correlation matrices and regression models.

### 2.5. Statistical Analyses

First, an exploratory analysis of the data was performed to visualize the distribution of soil properties at a depth of 0–40 cm, corresponding to the area effectively made usable (physically and chemically) by subsoiling. Violin plots, superimposed on individual values, were used to illustrate distribution density, dispersion, and unit observations [60]. For comparative and complementary purposes, the surface layer (0–10 cm) was also analyzed and presented in the Supplementary Materials. This visual step made it possible to identify dominant trends, detect possible extreme values, and assess the vertical stratification of soils before undertaking inferential statistical analyses.

In order to compare soil properties between the two depths studied (0–10 cm and 0–40 cm), a one-way analysis of variance (ANOVA) was performed for each parameter. The normality of the residuals was verified using the Shapiro–Wilk test [61]. When the normality assumption was not met ( $p < 0.05$ ), a nonparametric Wilcoxon–Mann–Whitney test was used as an alternative. The significance threshold was set at  $p < 0.05$ . The effect size ( $\eta^2$ , eta-squared) was also calculated to assess the magnitude of the difference observed between depths. The  $\eta^2$  values were interpreted according

to the thresholds proposed by [62], namely: small effect ( $\eta^2 < 0.06$ ), moderate effect ( $0.06 \leq \eta^2 < 0.14$ ), and large effect ( $\eta^2 \geq 0.14$ ). Comparative analyses between the 0–10 cm and 0–40 cm horizons (presented in Supplementary Materials, Table S1) indicate that only total organic carbon content and available phosphorus differ significantly between the two depths ( $p < 0.05$ ), with higher values at the surface. The other properties show no statistically significant differences, confirming the dominant role of parent material and subsoiling in the chemical structure of the 0–40 cm profile. These results support the choice of considering the 0–40 cm depth as the central functional zone for analyzing soil fertility and maize yield.

Given the high spatial heterogeneity observed for several soil properties, coefficients of variation (CV%) were calculated and added to the descriptive statistics presented in Table S1. This additional metric complements the minimum, maximum, mean, and standard deviation values, and allows a clearer assessment of the relative dispersion of each soil variable in this heterogeneous plinthic landscape. Potential extreme values in soil chemical properties were visually examined through violin plots and box-whisker distributions. No observations were removed, as all values were regarded as realistic within the natural pedological and geochemical variability of Plinthosols in the Lubumbashi region, where localized enrichment in metallic elements is common. Instead of excluding these values, non-parametric tests were applied when normality was not met, limiting the influence of skewed distributions while preserving the empirical variability of the dataset.

Beyond the univariate analysis, a multivariate approach was employed to explore the relationships between soil properties and identify the dominant pedogenetic processes structuring the site's variability. This analysis was applied mainly to data measured at a depth of 0–40 cm. As a supplement, the same analysis was also performed on data from 0 to 10 cm. The data were standardized beforehand, and the distance matrix was constructed using the metric  $1 - |r|$ , where  $r$  represents Pearson's correlation coefficient. This metric was chosen because it allows variables with similar behaviors to be grouped, regardless of the sign of their correlation, which is particularly relevant in tropical soils where antagonistic interactions between certain elements can coexist. Hierarchical classification was then performed using the average linkage method, recognized for its robustness and stability in the analysis of multivariate environmental data [63].

Next, to link soil characteristics to yield, and in order to ensure the statistical independence of observations and avoid pseudo-replication, maize yield was considered as a single value per block. Thus, for each block, the average of the yields obtained during the two growing seasons was calculated and used as the response variable in the analyses. This choice reduces the influence of seasonal fluctuations related to climatic or operational conditions and represents a yield that integrates the structural productive potential of the block rather than a cyclical effect. This average value was then used as the dependent variable for correlation analysis and multiple linear regression modeling.

On this basis, a correlation analysis and multiple linear regression modeling with stepwise selection were performed to identify the soil properties explaining the variability in average yield between blocks. A Spearman correlation matrix was first used to detect variables with a significant relationship to yield. The overall model was then constructed using stepwise selection (forward and backward), guided by the Akaike information criterion (AIC), to select the most optimal model [64,65]. Redundancy between variables was checked using the Variance Inflation Factor (VIF), with only those with a VIF  $< 3$  being retained [66,67]. The performance of the final model was evaluated using the coefficient of determination ( $R^2$ ), the root mean square error (RMSE), and the significance of the coefficients ( $p < 0.05$ ) [58].

The model predictors were constructed from soil properties measured at two functional depths: 0–10 cm, representing the surface horizon directly influenced by the termite mound amendment, and 0–40 cm, corresponding to the root zone actually exploited by maize after subsoiling. This dual approach allows for the integration of both the immediate effects of surface amendment and the physical and chemical conditions controlling root exploration at depth. The Depth<sub>0–40</sub> cm variable represents the exploitable depth of the soil before the appearance of a limiting layer (plinthite, stones, hardening, or heavy compaction) after subsoiling. This approach allows for the integration of the vertical continuity of the profile, unlike the exclusive use of the surface.

As the model is calibrated only with data measured between 0 and 40 cm, it is applicable within this range of validity. Thus, any greater depth observed in the field ( $>40$  cm) is reduced to 40 cm, as no empirical information is available beyond this limit. This choice avoids extrapolation

outside the domain, which is a source of bias in statistical models [68]. The yield prediction equation was expressed using unstandardized coefficients, while standardized beta coefficients and their 95% confidence intervals were used to compare the relative importance of the predictors [69]. All statistical analyses and figure generation were performed in R (version 4.5.1), using the tidyverse, broom, ggplot2, and FactoMineR packages (version 2.11) [70].

### 3. Results

#### 3.1. Distribution of Soil Physicochemical Properties at 0–40 cm

Figure 6 shows the distribution of the main physicochemical properties of the soil at a depth of 0–40 cm. The results indicate a high spatial heterogeneity of most parameters, reflecting the variability of edaphic conditions within the study area, which is characteristic of Plinthosols subject to marked morphological and water constraints.

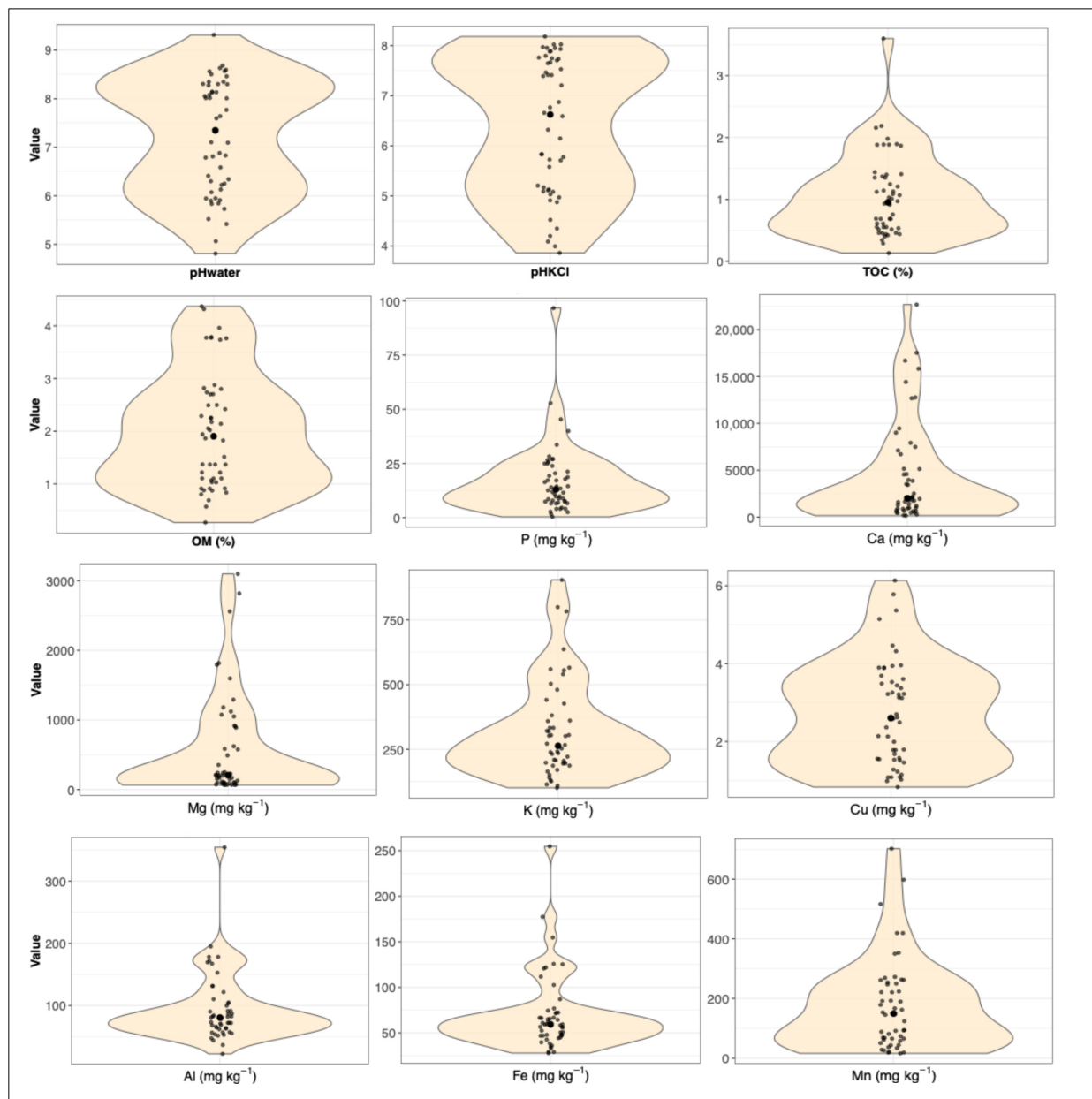


**Figure 6.** Distribution of soil physicochemical properties at 0–40 cm after subsoiling and amendment with termite mound materials at the study site. TOC refers to total organic carbon and OM to soil organic matter. Each point corresponds to an individual observation ( $n = 50$ ), while the width of the violin represents the probability density of the values for each variable analyzed.

The high Fe, Al, and Mn contents observed at this depth confirm the dominant influence of oxide-rich parent material, a signature of ferrallitization and plinthification processes. Conversely, available base cations such as Ca, Mg, and K, together with Cu, exhibit more widespread and spatially heterogeneous distributions within the 0–40 cm layer. These patterns indicate a stronger vertical variability in this functional zone compared with the surface horizon. Such distributions may be compatible with a partial vertical reorganization of elements within the profile; however, in the absence of control plots, no specific effect can be attributed to subsoiling or to the termite mound amendment. This heterogeneity suggests that the 0–40 cm layer functions as a chemically more contrasted rooting environment, which may influence nutrient accessibility for plants.

Detailed results for the surface layer (0–10 cm), a horizon directly influenced by farming practices and with a constant thickness, are presented in the Supplementary Materials for comparison (Figure S4).

In addition to the graphical exploration, the descriptive statistics further confirm strong spatial variability across the profile (Table S1). At 0–10 cm, total organic carbon (TOC) ranged from 0.4 to 2.3% (mean 1.4%), available P from 0.7 to 148.8 mg kg<sup>-1</sup> (mean 27.7 mg kg<sup>-1</sup>), and extractable Mn from 8.6 to 567.9 mg kg<sup>-1</sup> (mean 183.3 mg kg<sup>-1</sup>). Comparable variability was observed at 0–40 cm, where TOC ranged from 0.13 to 3.6% (mean 1.0%), available P from 0.35 to 96.7 mg kg<sup>-1</sup> (mean 17.1 mg kg<sup>-1</sup>), and extractable Mn from 5.9 to 702 mg kg<sup>-1</sup> (mean 177.1 mg kg<sup>-1</sup>). Comparisons between depths revealed significant vertical differentiation only for TOC and available P ( $p < 0.05$ ), with higher values in the surface layer, whereas all other properties showed no significant differences according to one-way ANOVA or Wilcoxon tests when normality was not met. Coefficients of variation (CV%) further confirmed high dispersion for several variables—particularly P, Mn, and Ca—indicating that spatial heterogeneity remains a dominant feature of these plinthic soils despite mechanical and chemical restoration efforts.

### 3.2. Relationships Between Soil Properties and Identification of Dominant Pedogenic Processes

The results of the hierarchical classification applied to the properties measured in the 0–40 cm horizon show the coexistence of three major pedogenetic processes structuring the current functioning of the Plinthosol after subsoiling and amendment with termite mound materials (Figure 7).

The first process groups available base cations (Ca, Mg, K), copper, and manganese together with soil pH, indicating a strong covariation among these variables. This pattern is consistent with the known role of basic cations in modulating soil acid–base status in highly weathered tropical soils. Although termite mound materials are typically enriched in Ca and Mg, the present observational design does not allow us to determine the extent to which their distribution results from the amendment, subsoiling, or pre-existing soil conditions. Nonetheless, the association between these cations and pH suggests a shared underlying pedochemical control influencing exchange complex saturation within the 0–40 cm layer. This process limits the excessive solubilization of manganese, a potentially toxic element in highly acidic conditions, and generally improves the chemical conditions in the rhizosphere. The presence of K and Cu within this group indicates that these nutrients exhibit similar spatial patterns to the base cations and pH. While termite mound materials are known to contain appreciable amounts of K and micronutrients, the observational nature of the study does not allow us to attribute their distribution specifically to the amendment or to subsoiling. Instead, their co-association suggests that these elements are governed by shared pedochemical factors influencing nutrient availability within the root-accessible layer.

The second process is mainly controlled by both total organic carbon (TOC) and organic matter (OM), which is closely associated with aluminum (Al). This grouping reflects a strong functional link between organic matter and aluminum dynamics in tropical acidic soils. Organic matter plays a key role in the complexation of Al<sup>3+</sup>, reducing its mobility and toxicity to roots. This mechanism is an essential lever in improving the functional fertility of Plinthosols, as it mitigates the harmful effects of aluminum toxicity while enhancing the soil's exchange capacity.

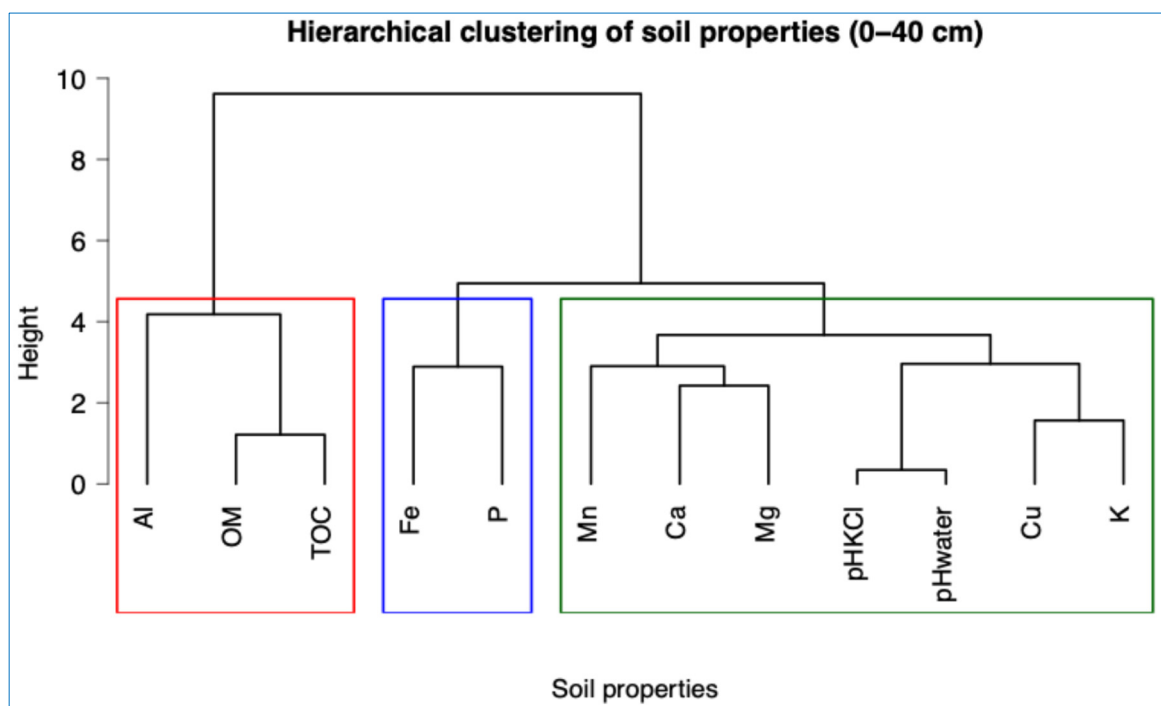


**Figure 7.** Hierarchical classification of physicochemical properties at 0–40 cm. The dendrogram represents the hierarchical classification of soil properties measured at this depth. The distance matrix was calculated using metric  $1 - |r|$ , based on Pearson's correlation coefficient, and groupings were performed using the average linkage method. Colored rectangles indicate the main clusters of soil properties corresponding to dominant pedogenic and functional processes discussed in the text.

Finally, the third process closely links iron (Fe) and phosphorus (P). This association reflects the control of phosphorus availability by iron oxides and hydroxides, a process characteristic of highly altered ferralitic and plinthic soils. The strong chemical affinity between P and Fe leads to phosphorus fixation, limiting its bioavailability to plants, despite measurable levels in the soil. This group thus reveals one of the major mechanisms constraining phosphate nutrition in these tropical systems.

Overall, the organization of variables in the dendrogram is not solely the result of statistical structuring, but reflects a coherent and hierarchical pedogenetic functioning at 0–40 cm. These results indicate that the soil properties measured within the 0–40 cm layer display a chemical and functional organization that is consistent with what would be expected in a less restrictive rooting environment. While the study design does not allow us to attribute this configuration specifically to subsoiling or to the addition of termite mound materials, the observed patterns suggest that the combined field interventions applied in this system are associated with a root zone that is less limiting for maize development.

The hierarchical classification at 0–10 cm (Figure S5) shows a broadly similar chemical organization, but with a stronger influence of surface amendment and cultivation practices. This comparison confirms that the dominant pedogenetic processes identified at 0–40 cm are already initiated at the surface, while their full functional expression emerges within the mechanically restored rooting zone.

### 3.3. Spatial Variation in Grain Maize Yield After Subsoiling and Spreading Termite Mound Material

Figure 8 illustrates the spatial distribution of grain maize yield across the entire study area for the two growing seasons (2022–2023 on the left, 2023–2024 on the right), after subsoiling and the addition of termite mound material. Yields vary greatly across the area, with values ranging from less than  $2.3 \text{ t ha}^{-1}$  to more than  $11.1 \text{ t ha}^{-1}$  depending on the zone. During the first season, distribution is heterogeneous: some blocks show low yields, while others achieve significantly higher levels, particularly in areas located in low-lying topographical positions near the river, where soil moisture is likely to be more favorable.

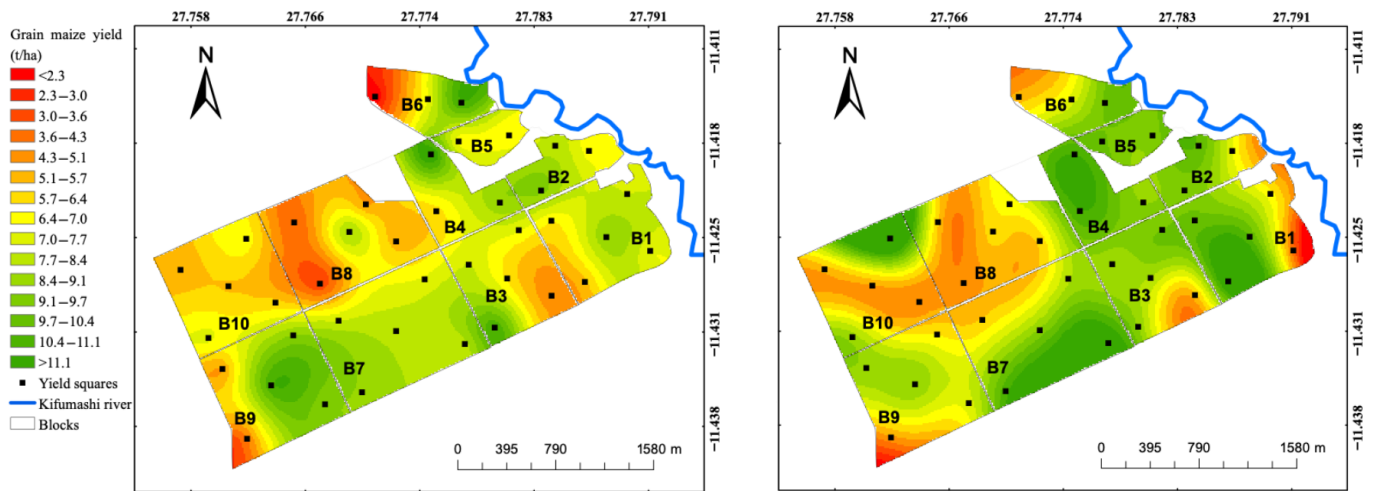


**Figure 8.** Spatial distribution of grain maize yield after subsoiling and addition of termite mound material. Left: 2022–2023 growing season and right: 2023–2024 growing season. B = blocks (B1–B10).

During the second season, there is a general improvement in yield in almost all blocks, with an average gain of about one ton per hectare. Blocks B8 and B10 continue to have lower yields overall, as in 2022–2023, but some sub-sectors within these blocks show considerable improvement. This trend suggests a cumulative effect of subsoiling and the addition of termite mound material, the impact of which increases as the amendments are incorporated into the soil profile.

### 3.4. Correlations Between Soil Properties (0–40 cm) and Average Maize Yield

The correlation heatmap summarizes the relationships between soil properties at 0–40 cm and mean maize yield following subsoiling combined with termite mound amendments (Figure 9). Yield shows weak to moderate positive correlations with pH ( $r = 0.15$  for pH water;  $r = 0.13$  for pH KCl), organic matter and total organic carbon ( $r = 0.30$  and  $r = 0.36$ ), as well as available P ( $r = 0.15$ ) and base cations such as Ca and Mg ( $r = 0.21$  and  $r = 0.11$ ). Although these coefficients indicate limited linear dependence, they consistently identify these parameters as the soil properties most positively associated with yield in the restored root zone.

Several strong internal correlations among soil properties are also evident. Extractable Cu shows a marked positive association with pH ( $r = 0.80$  for pH water;  $r = 0.78$  for pH KCl), while Mn displays a moderately positive association ( $r = 0.66$  and  $r = 0.65$ ). Organic matter and TOC are strongly negatively correlated with metals, particularly Cu ( $r = -0.91$ ), Mn ( $r = -0.75$ ), and Fe ( $r = -0.47$ ), indicating clear internal structuring among the soil properties measured at this depth. A strong positive correlation is also observed between Ca and Mg ( $r = 0.77$ ).

In contrast, correlations between yield and metals are negative, with Mn ( $r = -0.49$ ) showing the strongest association, followed by Al ( $r = -0.27$ ), Fe ( $r = -0.18$ ), and Cu ( $r = -0.14$ ). These patterns indicate that metallic elements remain among the soil properties most negatively associated with yield under the explored conditions. This indicates that yield variability in restored Plinthosols primarily reflects the combined influence of reduced acidity, increased effective rooting depth, and partial mitigation of metal-related constraints. Correlation patterns observed in the 0–10 cm surface layer (Figure S6) broadly mirror those found at 0–40 cm, but with consistently weaker coefficients, suggesting that surface chemistry alone does not fully explain yield variability and reinforcing the importance of the subsoiled layer as the effective root exploration zone.

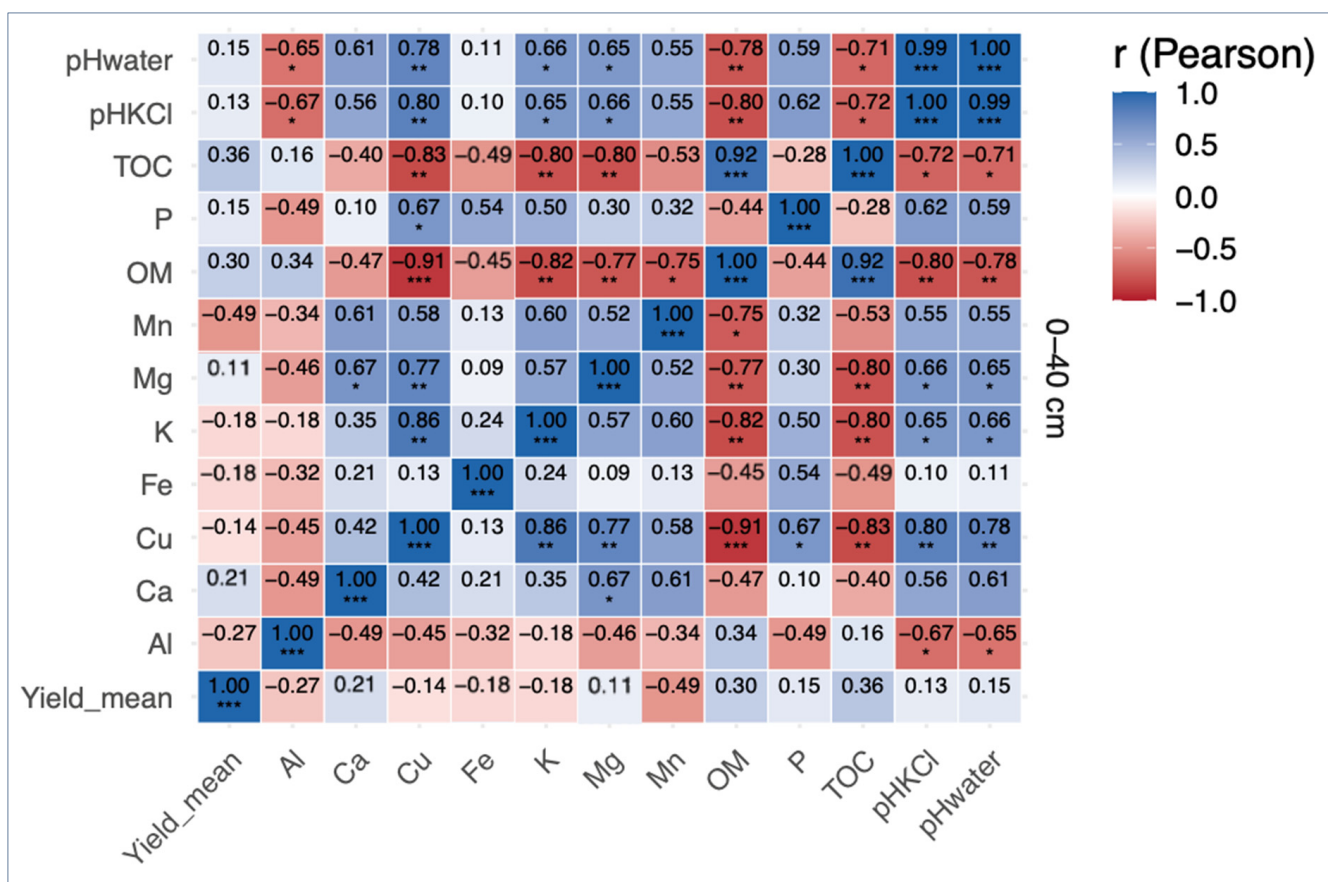


**Figure 9.** Correlation matrix between mean maize yield (Yield\_mean) and physicochemical properties at 0–40 cm. Each cell represents the Pearson correlation coefficient (*r*), illustrated by a color gradient (blue = positive correlation, red = negative correlation, white = no relationship). Asterisks indicate the level of statistical significance: \* *p* < 0.05; \*\* *p* < 0.01; \*\*\* *p* < 0.001.

### 3.5. Maize Yield Modeling: Multiple Linear Regression with Stepwise Selection

The stepwise model correctly predicts the observed maize yield, with an *R*<sup>2</sup> of 0.63 and an average error of 0.60 t ha<sup>-1</sup>, confirming a satisfactory correspondence between measured and estimated values (Figure 10a). Based on the selected predictors (depth<sub>0–40</sub>, pH(KCl), TOC, and Mn), the relationship between soil properties and maize yield can be expressed using the predictive Equation (Yield, Equation (4)):

$$Yield \left( t \text{ ha}^{-1} \right) = -1.03 + 0.11 \text{ Depth}_{0-40} + 0.87 \text{ pHKCl} + 2.62 \text{ TOC} - 0.1 \text{ Mn} \quad (4)$$

Visualization of the standardized beta coefficients clearly shows the relative weight of each variable in the model (Figure 10b). Among the predictors selected, total organic carbon (TOC) has the strongest positive influence on yield, with the highest standardized beta coefficient in the model, indicating that it is the most influential positive predictor of yield. This means that an increase in total organic carbon is associated with a proportional increase in yield, all other things being equal. KCl pH also has a marked positive effect, indicating that lower soil acidity is associated with higher yields. The variable depth<sub>0–40</sub> cm, representing soil conditions up to a depth of 40 cm, also contributes positively to yield. This confirms that blocks with usable soil at greater depths have higher yields. In contrast, extractable manganese is the only predictor with a negative coefficient. Its beta value (−0.69) indicates that high Mn content is associated with a decrease in yield, suggesting that Mn can be a limiting factor when its concentration becomes excessive.

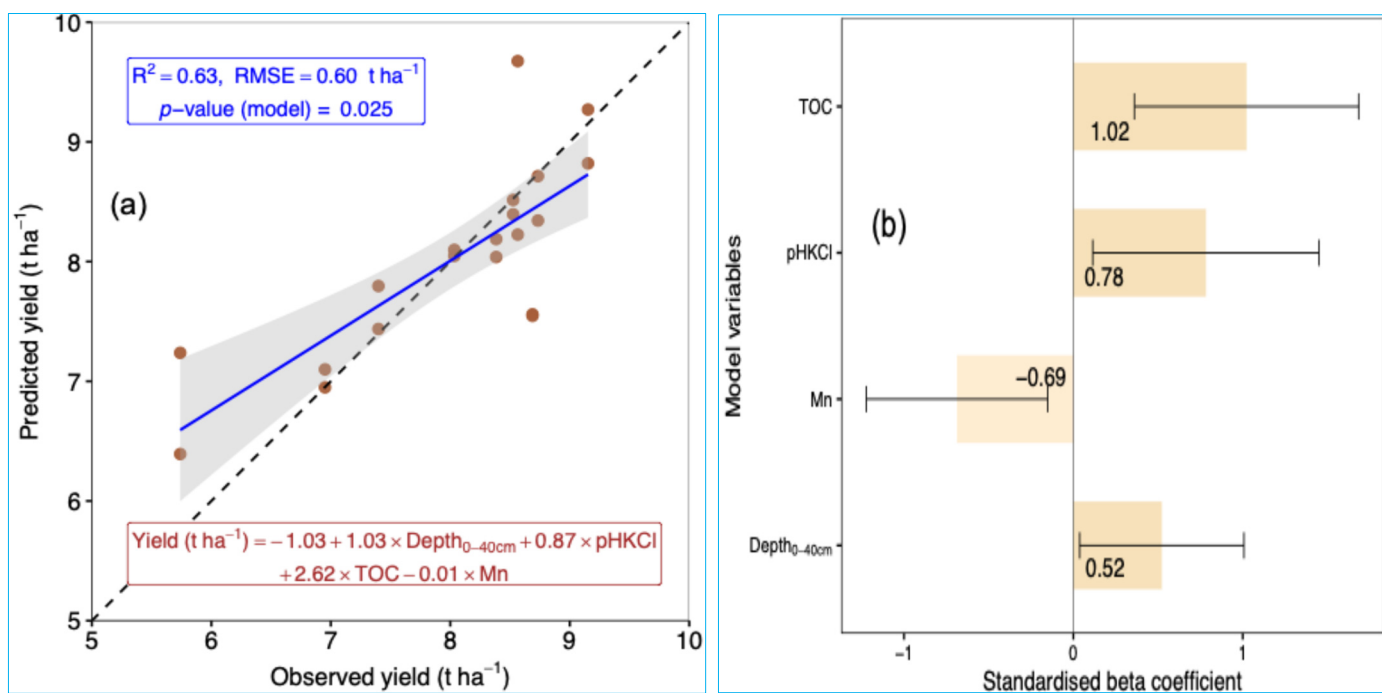


**Figure 10.** Final regression model explaining average maize yield ( $n = 20$ ). (a): relationship between observed and predicted average yield. The solid blue line represents the fitted linear regression, while the dashed black line indicates the 1:1 line (perfect agreement between observed and predicted values). (b): standardized beta coefficients of the selected variables, with their 95% confidence intervals. The 20 observations correspond to the 10 blocks for which the yield was obtained at two depths (0–10 cm and 0–40 cm). For each block, the yield used in the model is the average of the two growing seasons, ensuring the statistical independence of the data and avoiding any pseudo-replication.

## 4. Discussion

### 4.1. Distribution and Functional Significance of Physicochemical Properties at 0–40 cm

The distribution of soil physicochemical properties at a depth of 0–40 cm reflects significant spatial heterogeneity within the study area, reflecting the functional complexity characteristic of Plinthosols subject to both morphological constraints (irregular presence of plinthite) and targeted anthropogenic interventions (subsoiling and amendment with termite mound materials). This depth corresponds to the zone that is effectively made physically and chemically exploitable by maize thanks to subsoiling ( $\geq 40$  cm), making it a particularly relevant functional unit for interpreting the actual functioning of the profile and the edaphic processes influencing productivity. The relatively high concentrations of Fe, Al, and Mn observed at 0–40 cm suggest the expression of plinthite, which is characterized by high concentrations of Fe, Al, and Mn [48,71–73]. These redox-sensitive elements contribute to the stabilization of the mineral structure but also constitute potential chemical constraints, particularly through phosphorus fixation and aluminum or manganese toxicity under acidic conditions [1,74–76]. Their variability at this depth suggests heterogeneity in the degree of weathering and water dynamics within the profile, closely linked to the spatial distribution of plinthite.

Conversely, available cations ( $\text{Ca}^{2+}$ ,  $\text{Mg}^{2+}$ ,  $\text{K}^{+}$ ) and Cu display more widespread and heterogeneous distributions within the 0–40 cm layer. Such patterns suggest partial vertical redistribution of these elements, although the observational design of the study does not allow us to attribute these distributions specifically to subsoiling or to the addition of termite mound materials. Termite mound materials are known to be rich in fine clays, organo-mineral colloids, and basic cations, which can contribute to enriching the exchange complex and increasing cation exchange capacity [39,77–79]. Likewise, subsoiling is reported in the literature to break compacted horizons and enhance macropore continuity, thereby favoring percolation, solution movement, and deeper root exploration [28,80–83]. The patterns observed here are consistent with these mechanisms described in tropical soils, where

increasing the depth of soil effectively exploitable by roots is considered an agronomic lever as influential as chemical fertility enhancement [1–3,5].

Thus, the variability observed at 0–40 cm reflects not only the pedogenetic heritage of the soil but also the functional reconfiguration of the profile induced by the practices applied. This level then becomes a hybrid soil compartment, marked both by the geochemical signature of the parent plinthic material and by the secondary effects of soil amendment and deep tillage. This transformation largely explains why the exploitable depth appears as a structuring variable in subsequent analyses, particularly in the regression model explaining maize yield.

The results for the surface layer (0–10 cm), which is directly influenced by cultivation practices and has a more consistent thickness across the site, are presented in Supplementary Materials (Figure S1) for comparison. Their analysis confirms the vertical consistency of the profile's functioning while reinforcing the relevance of choosing the 0–40 cm depth as the central reference for the agronomic and pedological interpretation of this study.

A limitation of this study is the absence of untreated control plots and pre-intervention baseline measurements, which prevents direct causal attribution of the observed soil and yield patterns to the management practices. Consequently, our interpretation focuses on spatial variability and soil–yield associations within the mechanically loosened depth (0–40 cm), in line with mechanisms described in the literature for plinthic and ferrallitic soils. In addition, while this concentration-based approach allows for a detailed characterization of soil chemical dynamics, a more comprehensive assessment of biogeochemical functioning could be obtained by calculating nutrient stocks. Such an approach, integrating the measured concentrations, bulk density, and actual usable depth at each point, would be a relevant way to better quantify the effective nutrient reserves in this highly spatially heterogeneous landscape and to refine long-term management recommendations for cultivated Plinthosols.

Moreover, because no control plots without subsoiling and/or without termite mound amendment were available, the respective contributions of mechanical loosening and chemical enrichment cannot be disentangled. As a consequence, the observed variations in rooting depth, soil chemical properties and maize yield should be interpreted as associations characterizing the soil conditions under the current management system, rather than as causal effects attributable to either practice individually or to their combined action. While the reduced stratification of nutrients and the progressive yield increase across seasons are consistent with the combined influence of subsoiling and termite-derived amendments, these trends cannot be conclusively assigned to one intervention independently. Therefore, our interpretation focuses on the agronomic consequences of restoring a mechanically and chemically exploitable rooting depth, acknowledging that the relative weight of each component remains unresolved in the absence of non-intervened controls.

Although available nutrients in this study were extracted using the ammonium acetate–EDTA (AAAc-EDTA) method at pH 4.65, which is widely applied in acidic tropical soils [54], it is important to acknowledge that the extraction efficiency and selectivity of this method can change as soil pH increases due to amendments. In particular, the incorporation of termite mound materials—rich in basic cations such as Ca, Mg, and K—can locally raise soil pH [39,84], reducing the extractability of some nutrients by AAAc-EDTA and affecting the relative responses of individual elements. Under these conditions, alternative extractants such as Mehlich-3 [85] or Olsen bicarbonate [86] have been shown to provide more consistent estimates of plant-available phosphorus and cationic micronutrients across a broader pH range. Nonetheless, AAAc-EDTA was retained in the present study to maintain comparability with regional soil databases and because most samples remained within acidic to moderately acidic conditions. Future research should include comparative extractions (AAAc-EDTA vs. Mehlich-3/Olsen) to evaluate how changes in pH following termite mound amendment may influence the interpretation of nutrient availability and fertility status.

#### 4.2. Organization of Soil Properties and Dominant Pedogenic Processes

Analysis of the hierarchical classification carried out on the properties measured in the 0–40 cm horizon shows the existence of three major pedogenetic processes that structure the current functioning of the Plinthosol after subsoiling and amendment with termite mound materials. The first process is dominated by available base cations (Ca, Mg, and K), associated trace metals (Cu and Mn), and soil acidity indicators (pH in water and KCl), reflecting an acid–base regulation process typical of tropical soils enriched in basic cations. This structure reflects direct control of the soil's

acid-base status through the enrichment of basic cations linked to the incorporation of termite mound materials. These materials, known for their richness in fine clays and exchangeable bases, help to increase pH, improve cation exchange capacity, and rebalance the adsorbing complex in initially very acidic soils [17,39,40,77,87,88]. The increase in Ca and Mg promotes gradual deacidification of the environment and limits the excessive solubility of Mn, an element that can become phytotoxic [89–91] under the acidic conditions characteristic of unamended Plinthosols. This close relationship between pH, available base cations, and Mn therefore reflects a chemical regulation process induced by the amendment, contributing to the creation of a soil environment that is less restrictive for root development. The presence of Cu and K in this process reinforces the hypothesis of direct enrichment of the root zone with essential nutrients, linked to bioturbation and the vertical redistribution of termite mound materials after subsoiling.

The second process is structured around organic matter, total organic carbon, and aluminum. This association reveals the central role of organic matter in regulating aluminum toxicity in acidic tropical soils [1]. Organic matter can complex  $Al^{3+}$  through organo-metallic bonds, thereby reducing its mobility and availability in a form that is toxic to roots [1,92–94]. This complexation helps to reduce chemical stress on the root system and improve conditions for water and nutrient absorption [95]. In addition, the increase in organic matter, stimulated by the addition of termite mound material rich in stabilized organo-mineral compounds, improves the soil's buffering capacity, structure, and exchange capacity [96–98]. This process, therefore, plays a fundamental role in improving the functional fertility of Plinthosols, helping to simultaneously reduce acidity and aluminum toxicity, two major constraints on maize yield in these tropical environments [1].

The third process closely links iron and phosphorus, confirming that P availability is controlled by the oxide phases of the subsoil [74]. In plinthic soils, Fe and Al oxides have a strong chemical affinity for P and can immobilize it through ligand exchange bonds [1,75]. This interaction explains why, despite the measurable presence of phosphorus in the soil, its availability to plants remains limited, thus constituting a persistent constraint on the phosphorus nutrition of maize. Subsoiling, although it does not directly alter the chemical affinity between Fe and P, does allow roots to explore a larger volume of soil, thereby increasing the likelihood of accessing areas where phosphorus can be locally mobilized. This process suggests that yield improvement is not solely dependent on increased nutrient concentrations but also on an expansion of the functional soil volume accessible to the root system.

Thus, the organization of variables observed in the dendrogram is not a simple statistical result: it reflects a change in the pedogenetic status of the soil, which is evolving toward a less acidic state, better supplied with available base cations, less constrained by aluminum toxicity, and characterized by a deeper and more functional root zone. This evolution reflects a transition from Plinthosol to an agropedological functioning more favorable to nutrient absorption and, consequently, to a sustainable increase in maize productivity. The results corresponding to the 0–10 cm depth, characterized by a more constant thickness but a more direct influence of surface cultivation practices, are presented in Supplementary Materials (Figure S2) for comparison and confirm the vertical consistency of the observed pedogenetic functioning.

However, the identification of these dominant pedogenetic processes suggests that spatial mapping of these mechanisms could be considered in future work. Such an approach would make it possible to better discriminate, at the plot level, between areas with high agronomic potential and those subject to major pedochemical constraints in order to more finely target management and amendment practices for Plinthosols.

#### 4.3. Spatial Variability in Yield After Subsoiling and Amendment

The high spatial heterogeneity of observed yields ( $2.3$  to  $11.1$  t ha<sup>-1</sup>) reflects the strong spatial variability of soil conditions across the site. These patterns are consistent with the fact that subsoiling and termite mound amendments had been implemented operationally across the study area; however, in the absence of untreated control plots, the study cannot attribute this heterogeneity directly to either intervention. These values are significantly higher than the regional averages typically reported for maize in Haut-Katanga, where farmers obtain less than  $1$  t ha<sup>-1</sup> under traditional practices [11,99], and they also exceed the upper range generally achieved in improved systems relying primarily on fertilization, varietal improvement and genetic progress ( $\approx 1.5$ – $8.5$  t ha<sup>-1</sup>; [9,99–102]). This sug-

gests that restoring the exploitable rooting depth can unlock yield levels beyond those commonly reachable through nutrient enrichment alone. Thus, our findings reinforce previous work showing that increased rooting depth is a primary determinant of maize performance under compacted soils [26,35,46,103,104], while extending current knowledge by demonstrating that gains can surpass those obtained through fertilization alone when chemical and physical restoration act together.

No laboratory characterization of termite mound materials was performed in this study, as sampling occurred after their incorporation during operational fieldwork. However, previous analyses conducted in the same region indicate that these materials are generally enriched in fine clays, Ca, Mg, K, Fe and exchangeable bases [13,33,77,84], supporting their potential to enhance soil chemical status. These findings align with reports showing that termite-derived amendments contribute to structural stabilization and gradual nutrient enrichment [17,41,42,87]. Our results are consistent with the direction of chemical improvement reported in earlier studies. They further indicate that, within the studied system, higher yields are associated with soil conditions observed in areas where termite mound materials and subsoiling were jointly applied. However, in the absence of untreated control plots, these yield levels should be interpreted as spatial patterns emerging from the combined management context rather than as effects attributable to chemical enrichment alone or to any specific practice.

The highest yields correspond to blocks where exploitable rooting depth was more fully restored, enabling three-dimensional root exploration and greater access to subsurface nutrients and water. In low-lying positions near the river, water availability likely amplified this effect by reducing drought stress during critical growth stages. This spatial behavior is consistent with studies showing that increased root depth enhances resilience under restrictive physical conditions [37,105,106] and that subsoiling improves macroporosity, water percolation and deep water recharge [82,107–109]. Thus, yield improvement arises not only from chemical fertility but also from structural modification of the soil that fundamentally alters resource accessibility. Importantly, the maximum yields observed here ( $>10 \text{ t ha}^{-1}$ ) exceed values commonly reported in Ferralsols without deep mechanical intervention [6,110,111], supporting the hypothesis that restoring exploitable depth may raise the physiological ceiling of maize productivity in these environments.

Similar functional constraints have been documented by Nikkel & Lima [112], who demonstrated that plinthite ironstone concretions reduce gas exchange, vegetative growth, and phenological development in maize even when nutrients are sufficient. Although their study did not quantify grain yield directly, the observed reductions in plant height and biomass indicate that mechanical limitations to rooting can suppress crop performance independently of chemical fertility. In contrast, the high yields obtained in the present study—particularly where exploitable rooting depth was fully restored—suggest that subsoiling alleviated these growth constraints and enabled maize to realize a higher productive potential. This comparison reinforces the interpretation that physical restriction of rooting depth is a primary bottleneck for maize productivity in plinthic environments and that depth restoration can unlock yield levels that are not attainable through nutrient enrichment or genetic progress alone.

The increase in yield observed from the first to the second season coincides with relatively comparable climatic conditions between seasons. This temporal pattern suggests that yield levels evolved within a stable climatic context and may reflect progressive changes in soil conditions across seasons. However, in the absence of untreated control plots, this inter-seasonal increase cannot be attributed to cumulative or delayed effects of subsoiling or termite mound amendments but should instead be interpreted as a temporal expression of the managed system as a whole [15,43,97,113]. Comparable time-lag effects have been observed in tropical soils amended with organo-mineral inputs [76,111], and our study extends this understanding to restored plinthic soils.

Beyond intrinsic plinthic heterogeneity, the strong yield variability among blocks likely reflects interactions between past management (legacy effects) and recent restoration. Previous studies show that historical differences in fertilization and tillage can persist and modulate crop responses even after intervention [1,111,114,115]. Our results confirm this persistence while extending current knowledge by demonstrating that such legacies condition the agronomic expression of restored rooting depth. Together, these findings indicate that sustained yield improvements in plinthic tropical soils require not only physical loosening and chemical amendment but also progressive harmonization of management practices to reduce block-to-block disparities.

#### 4.4. Influence of Soil Properties on Maize Yield Variability

Correlation analysis between soil properties at 0–40 cm, the depth effectively made usable by the maize root system after subsoiling, highlights the main chemical and functional factors controlling productivity in Plinthosols amended with termite mound materials. Unlike a strictly superficial approach, this depth integrates both the mechanical effect of subsoiling on root volume and the chemical effect of the amendment on the functional fertility of the profile.

The positive correlations observed between maize yield, soil pH (water and KCl), and organic matter content (OM, TOC) confirm that reducing acidity and enriching carbon are essential levers for productivity in these highly constrained soils. In Plinthosols, low pH is generally associated with increased solubility of aluminum and manganese, two elements that are phytotoxic to roots [92,116]. The increase in pH observed within the 0–40 cm layer is associated with higher concentrations of Ca and Mg and coincides with improved chemical conditions in the rhizosphere. This pH environment is generally considered more favorable for root functioning and nutrient availability; however, in the absence of untreated control plots, this pattern cannot be causally attributed to the addition of termite mound materials or subsoiling alone.

The positive correlation observed between soil pH and extractable Cu in our dataset likely reflects the strong influence of organic matter and colloidal surfaces on Cu dynamics. Higher pH favors the formation of Cu–organic complexes and enhances adsorption onto reactive surfaces, which can maintain Cu in extractable but non-free ionic forms [117–119]. This mechanism may explain why extractable Cu does not decrease with increasing pH in our case, despite the commonly reported inverse relationship between pH and metal solubility in acidic tropical soils. However, because most studies have documented a reduction in Cu solubility with increasing pH in the absence of strong organic complexation, further targeted investigation would be required to disentangle the relative contributions of organic matter, pH buffering, and amendment-related inputs in this Plinthosol system. Such work could clarify whether the observed trend is specific to the amendment strategy used here or reflects a broader pedochemical behavior of Cu in amended plinthic soils. In our dataset, soil pH (water/KCl) displays a strong positive association with extractable Cu ( $r = 0.80/0.78$ ) and a moderately positive association with extractable Mn ( $r = 0.66/0.65$ ), whereas no meaningful relationship is observed for Fe ( $r = 0.10/0.11$ ). These contrasted responses are consistent with the element-specific mechanisms governing metal speciation in weathered tropical soils [1]. The marked sensitivity of Cu and Mn to pH likely reflects enhanced sorption and organo-complexation at higher pH values, which maintain these elements in extractable, yet predominantly non-free ionic forms [119–121]. In contrast, Fe mobility remains largely controlled by redox-driven dissolution–precipitation cycles of Fe-(oxyhydr)oxides rather than by proton activity alone [122]. This differential behavior provides a mechanistic explanation for the persistence of Cu- and Mn-related yield constraints despite partial acidity mitigation, while the weaker pH dependence of Fe helps account for its negligible statistical influence on yield variability in this system.

The positive correlation between yield and total organic carbon also highlights the structuring and functional role of organic matter in this system. Not only does it improve cation exchange capacity, but it also acts as a complexing agent for potentially toxic metals, reducing their mobility and bioavailability [95,123]. The strong negative correlation between organic matter and certain elements such as Mn, Fe, and Cu shows that organic matter plays an essential buffering role in controlling metal toxicity within the root zone restructured by subsoiling, reflecting the role of organic matter in complexing and stabilizing these metals, reducing their bioavailability [124,125]. Mujinya et al. [33] add that the presence of organic matter can lead to the formation of complexes with metals such as aluminum and iron and contributes to the overall cation exchange capacity of the soil, which affects the retention of metal cations. Thus, at this depth, organic amendments act as fertility regulators and barriers against metal toxicity.

The positive, albeit moderate, correlations observed between yield and available base cations (Ca and Mg) confirm that these elements not only play a nutritional role but also contribute to acidity neutralization and aluminum desaturation of the exchange complex. In highly acidic soils, calcium and magnesium act as chemical antagonists to aluminum, reducing its fixation on exchange sites and limiting its absorption by roots [92]. Their increased presence in the 0–40 cm zone is observed within the depth that is mechanically loosened and functionally accessible to the maize root system. However, in the absence of untreated control plots, this pattern cannot be attributed

to the amendment, to subsoiling, or to their combined effect and should be interpreted as a spatial association rather than a causal response.

Conversely, the negative correlations observed between yield and Al, Fe, Cu, and Mn confirm that, despite the restoration practices implemented, the mineralogical signature of plinthitic material remains a significant constraint in certain areas of the profile. These elements, which are abundant in ferrallitization and plinthification processes, can become phytotoxic when their concentration and solubility increase, particularly in microenvironments that are still highly acidic or poorly desaturated [48,126,127].

A comparable pattern concerns aluminum. In this study, ammonium acetate–EDTA extractable Al concentrations range from 24.3 to 201.6 mg kg<sup>-1</sup> at 0–10 cm and from 26.5 to 225.4 mg kg<sup>-1</sup> at 0–40 cm, with respective means of 85.4 mg kg<sup>-1</sup> and 94.9 mg kg<sup>-1</sup> (Table S1). Although extractable concentrations alone do not define a critical phytotoxicity threshold, the literature generally reports that phytotoxic effects in maize emerge when the exchangeable Al<sup>3+</sup> fraction exceeds ~1–2 cmolc kg<sup>-1</sup> ( $\approx$  90–180 mg kg<sup>-1</sup>), particularly under acidic conditions that sharply increase biologically active Al [128,129]. Although extractable soil Al concentrations alone cannot define a toxicity threshold, experimental work on maize indicates that phytotoxic effects emerge when root tissue Al reaches 13 mg kg<sup>-1</sup> (dw), corresponding to reduced root elongation and biomass [130]. In our case, soil pH values are predominantly near neutral, suggesting that most of the measured Al is likely complexed with organic matter or adsorbed onto Fe/Al oxides, thereby reducing its occurrence as free phytotoxic Al<sup>3+</sup>.

This interpretation is consistent with the moderate negative correlation observed between aluminum and yield at 0–40 cm ( $r = -0.29$ ): aluminum remains an agronomic constraint, yet less influential than manganese ( $r = -0.49$ ). This difference likely reflects the partial mitigation of Al toxicity following the increase in pH and organic matter associated with the amendments, which reduces the proportion of exchangeable Al<sup>3+</sup> and limits root growth inhibition. However, the occurrence of locally high concentrations combined with small-scale pH variability implies that episodes of aluminum toxicity cannot be entirely ruled out, particularly in microsites with low buffering capacity and low organic matter content. As with Mn, future work quantifying exchangeable or soluble Al would be required to determine the extent to which aluminum still contributes to soil constraints limiting maize productivity in this restored system.

Manganese shows a comparable behavior but with a stronger agronomic influence. It exhibited strong spatial variability, ranging from 8.6 to 567.9 mg kg<sup>-1</sup> at 0–10 cm and 15.9 to 702.0 mg kg<sup>-1</sup> at 0–40 cm, with mean values of 183.3 mg kg<sup>-1</sup> and 177.1 mg kg<sup>-1</sup>, respectively (Table S1). These concentrations fall mostly within the range considered adequate to moderately high for maize (~30–250 mg kg<sup>-1</sup>, [121,128]), but local “hotspots” clearly exceed commonly reported phytotoxic thresholds (~250–300 mg kg<sup>-1</sup>). Such elevated values may induce toxicity under acidic or poorly buffered conditions that increase Mn solubility and plant uptake [131,132].

While Mn extractability was determined using AAAC-EDTA, this extractant primarily reflects a potentially plant-available pool rather than the fraction that is actually taken up by roots or directly phytotoxic. In plinthitic and highly weathered tropical soils, Mn solubility and plant uptake are strongly modulated by moisture- and redox-driven dynamics: reducing conditions during wet phases increase the availability of Mn<sup>2+</sup> through the reduction of Mn oxides (Mn<sup>4+</sup>, Mn<sup>3+</sup>), whereas drying promotes re-oxidation and immobilization, limiting its availability to roots [133]. Because such temporal fluctuations were not captured in this study—sampling was conducted at a single time point and no Mn concentrations were measured in plant tissues—the observed negative association between Mn and yield should be interpreted as an indicator of potential Mn-related stress rather than direct confirmation of toxicity [134]. These redox-driven changes in Mn availability suggest that season-dependent solubility pulses may transiently increase Mn-related constraints in maize, beyond what can be inferred from single-time-point soil concentrations. Future work quantifying Mn speciation under contrasting moisture conditions, combined with Mn concentrations in plant tissues, would help determine whether reduced yield reflects direct toxicity, nutrient imbalance, or transient redox-driven pulses of Mn availability.

The significant negative correlation between Mn and yield ( $r = -0.49$ ) therefore indicates that Mn already acts as an agronomic constraint in the mechanically loosened rooting zone (0–40 cm), despite average concentrations remaining close to sub-toxic levels. This suggests that subsoiling

combined with termite-derived amendments reduced Mn solubility through partial acidity mitigation but did not fully eliminate Mn-related stress. Future research quantifying Mn speciation under contrasting moisture conditions, together with Mn concentrations in plant tissues, would more clearly discriminate between direct toxicity and nutrient-interaction effects. Work by Ji et al. [45] has shown that when mechanical constraints are removed by deep subsoiling, the maize root system can extend its exploration to approximately 35–40 cm, thereby significantly increasing the volume of soil explored for water and nutrients. This restored functional depth in decompacted Plinthosols fully justifies the integrated analysis of the 0–40 cm layer in the present study.

However, the fact that these correlations are observed in the 0–40 cm zone, currently accessible to roots thanks to subsoiling, indicates an essential point: yield improvement does not depend solely on the chemical composition of the soil, but above all on the ability of the root system to explore a larger volume of soil. Subsoiling has broken the physical constraints associated with plinthitis, increasing the exploitable root volume and allowing maize to access previously inaccessible water and nutrient reserves [82,107,109]. Thus, the relationship between soil properties at 0–40 cm and maize yield reflects a real change in the functioning of the soil–plant system. The observed productivity results from the interaction between (i) a reduction in chemical toxicity, (ii) an improvement in soil organo-mineral status, and (iii) an increase in the volume of soil effectively exploited by the roots.

The correlations observed in the 0–10 cm layer, presented in the Supplementary Materials (Figure S3), show patterns similar to those identified at 0–40 cm and indicate a more homogeneous distribution of soil properties near the surface. However, in the absence of untreated control plots, this homogenization cannot be attributed specifically to the addition of termite mound materials and should be interpreted as a spatial association within the managed system rather than as a direct causal effect.

#### 4.5. Stepwise Regression: Depth as a Direct Determinant of Yield

The multiple linear regression model constructed in this study has a coefficient of determination of 0.63 and an average error of  $0.60 \text{ t ha}^{-1}$ , which is a satisfactory performance for agronomic data obtained under real field conditions. In environments subject to high spatial heterogeneity, the literature indicates that an  $R^2$  between 0.40 and 0.60 is generally considered satisfactory [135]. Here, an  $R^2$  of 0.63 means that nearly two-thirds of the observed yield variability between blocks is explained by soil variables, which gives the model strong explanatory power for a complex edaphic system such as plinthic soils. This level of explicability is all the more remarkable given that no climatic or agronomic management variables (seed density, weed control, water stress) were included, suggesting that soil properties are one of the major determinants of yield in this pedological context.

The reliability of the statistical model is based not only on its performance ( $R^2 = 0.63$ ) but above all on the rigor of the process that led to the selection of predictors. In highly altered tropical soils, where physicochemical properties are often interdependent (pH—available cations—organic matter—metals), the major risk is multicollinearity, which produces unstable models and coefficients that are impossible to interpret correctly [136]. To circumvent this bias, the model was constructed using a strategy of progressively reducing the explanatory space: only the monotonic relationship between yield and soil properties was first verified via a robust correlation with non-normal distributions (Spearman), before the Akaike information criterion (AIC) automatically selected the combination of variables that best explained yield while penalizing redundant variables [64,65]. A final filter using the variance inflation factor ( $VIF < 3$ ) allowed independent predictors to be retained, ensuring the numerical stability of the model and the validity of the estimated coefficients, an approach recommended to avoid overfitting in environmental models [66,137]. Thus, the model does not describe a simple statistical correlation: it identifies soil variables whose effect on yield is real, non-collinear, and agronomically interpretable.

The use of standardized beta coefficients enhances the interpretability of the model by quantifying the relative influence of each variable independently of its unit of measurement [69]. This process revealed the importance of organic carbon, KCl pH, exploitable depth, and manganese in the model. Organic carbon appears to be the most influential predictor of yield. This result is consistent with the functioning mechanisms of highly altered soils, in which organic matter is the main source of exchange complex loads and therefore the main lever of fertility [1]. The role of KCl pH confirms that

acidity is a major limiting factor for yield, as it controls the solubility of aluminum and manganese, two elements that become toxic when pH decreases [123,124].

The exploitable depth (0–40 cm) is a particularly interesting agronomic variable in this model. It does not act as a simple classification factor but as a quantitative predictor reflecting functional root volume. Each increase in exploitable depth results in an increase in the volume of soil explored by the root system and therefore an increase in the water and nutrient reservoir. Several studies show that increasing the exploitable soil depth can increase crop yields by up to 70%, depending on the initial level of stress [19,25,107,109,138,139]. The fact that depth is a predictor automatically retained by the statistical model confirms that agronomic interventions (subsoiling + termite amendment) have permanently altered the functioning of the root system by creating a continuous exploitable horizon.

The negative influence of manganese, the last significant predictor in the model, adds a dimension of soil toxicology that is rarely included in agronomic models. The fact that Mn remains present in the final model despite strict selection by AIC and VIF indicates that its effect on yield is real, direct, and independent of other soil properties. This result is consistent with observations that manganese becomes phytotoxic under acidic conditions, reducing root elongation and disrupting leaf enzyme mechanisms [89–91,140,141]. Stoyanova et al. [116] observed a reduction in leaf chlorophyll and stunted growth in maize due to manganese toxicity. The combination of organic surface enrichment and a gradual reduction in acidity through deep tillage is therefore an effective lever for reducing this risk of toxicity.

The model's performance is also based on the methodological choice to use the average yield of the two growing seasons for each block. This decision eliminates pseudo-replication and ensures the statistical independence of the observations, a necessary condition for the use of linear models [142,143]. By doing so, the model not only captures a one-off statistical relationship but also highlights a more robust and reproducible agronomic relationship over time, implicitly integrating part of the interannual variability. However, the future integration of climatic variables (rainfall, temperature,  $ET_0$ ), as well as agronomic parameters (seed density, residue management, water stress), would further refine the predictive model, improve its accuracy, and strengthen its ability to be generalized to other similar agro-pedological contexts.

The sequential procedure, consisting of correlation screening, AIC-based variable selection, and VIF filtering, is well suited to highly interdependent tropical soils, as it isolates interpretable predictors and reduces collinearity-driven artifacts, thereby strengthening agronomic interpretation. However, this approach may also suppress weak interactions that could become relevant under different environmental conditions, and its reliance on linear relationships may underestimate non-linear or threshold-based responses. Thus, while the data-mining process provides a robust explanatory framework for identifying key soil determinants of yield, complementary approaches such as factorial field trials or time-series analysis would be required to fully assess causal pathways and capture temporal variability.

## 5. Conclusions

This study shows that, across blocks, plinthosols managed with subsoiling and termite mound amendments exhibit spatial associations between a deeper functionally exploitable rooting zone, higher maize yields, and changes in soil vertical organization, acidity, organic carbon content, and aluminum and manganese constraints. However, in the absence of untreated control plots, these patterns should be interpreted as co-occurring spatial trends within the managed system rather than as demonstrated causal effects of either practice. As a result, yields reached levels that are not only well above regional averages but also exceed those commonly reported in improved systems, demonstrating that restoring exploitable rooting depth can raise the productivity ceiling of Plinthosols.

The pedological dynamics observed are dominated by three structuring mechanisms: (i) acid–base regulation and enrichment in base cations; (ii) aluminum complexation by organic matter; and (iii) the control of phosphorus availability by iron oxides. The regression model confirms that exploitable depth, total organic carbon, and pH are the main determinants of yield, while manganese remains a limiting factor. These findings directly address the three research questions: restoring exploitable depth improves yield; specific soil properties—particularly pH, organic carbon, and

Mn—explain the observed spatial variability; and structural and chemical effects interact over time to reinforce productivity.

The main limitations of this study concern the absence of untreated control plots and the single-time-point sampling, which do not allow the contributions of subsoiling and termite mound amendment to be assessed at all, nor the seasonal fluctuations of Mn driven by redox cycles to be captured. Future work integrating factorial experiments, the quantification of nutrient stocks, climatic and hydrological data, as well as Mn concentrations in plant tissues, would strengthen causal interpretation and enhance the predictive capacity of the models. Finally, mapping the identified pedogenetic processes could support more targeted and sustainable management of Plinthosols in Haut-Katanga.

**Supplementary Materials:** The following supporting information can be downloaded at: <https://www.mdpi.com/article/10.3390/environments13010052/s1>, Figure S1. Semivariogram of observed grain maize yield and kriging-predicted yield for the first growing season. Figure S2. Semivariogram of observed grain maize yield and kriging-predicted yield for the second growing season. Figure S3. Performance evaluation of the interpolation methods based on root mean square error (RMSE) and bias for maize grain yield in the study area. NN: Natural Neighbor and SWB: Spline With Barriers. Figure S4. Distribution of soil physicochemical properties at 0–10 cm after subsoiling and amendment with termite mound materials at the study site. Figure S5. Hierarchical classification of physicochemical properties at 0–10 cm. The dendrogram represents the hierarchical classification of soil properties measured at this depth. (average linkage). Figure S6. Correlation matrix between average maize yield (Yield\_mean) and physicochemical properties at 0–10 cm. Table S1. Comparison of soil physicochemical properties between the two depths (0–10 cm and 0–40 cm) after subsoiling and amendment with termite mound material. For each variable, the following are presented: the minimum (min), maximum (max), mean, standard deviation (sd), coefficient of variation (CV), one-way ANOVA result (p\_anova), effect size ( $\eta^2$ ), Wilcoxon–Mann–Whitney test *p*-value when data do not follow normality (p\_wilcox), and Shapiro–Wilk test *p*-value (Shapiro\_p).

**Author Contributions:** Conceptualization, J.B.M., G.C. and E.K.L.M.; methodology, J.B.M., J.M., Y.U.S. and G.C.; sampling, J.B.M. and E.K.L.M.; software, J.B.M. and J.M.; validation, J.W., J.M., E.K.L.M. and G.C.; formal analysis, J.B.M.; resources, J.W., Y.U.S., E.K.L.M. and G.C.; data curation, J.B.M.; writing—original draft preparation, J.B.M.; writing—review and editing, J.B.M., J.M., Y.U.S., J.W., E.K.L.M. and G.C.; visualization, J.W., J.M., Y.U.S. and G.C.; supervision, E.K.L.M. and G.C.; project administration, E.K.L.M. and G.C.; funding acquisition, G.C. All authors have read and agreed to the published version of the manuscript.

**Funding:** This research was funded by the Académie de Recherche et d’Enseignement Supérieur (ARES-CCI) through the B-Mob grant, as well as by the PACODEL Impulse grant, Belgium.

**Data Availability Statement:** The data presented in this study are available on request from the corresponding authors.

**Acknowledgments:** The authors thank the Académie de Recherche et d’Enseignement Supérieur (ARES-CCI) for the doctoral scholarship awarded to John Banza Mukalay within the framework of development co-operation. We also extend our gratitude to the management of FarmCo MMG, particularly Deo Mwamba and Célestin Nkulu, for providing the study site and support during the research.

**Conflicts of Interest:** The authors declare no conflicts of interest.

## References

1. Sanchez, P.A. *Properties and Management of Soils in the Tropics*; John Wiley & Sons: New York, NY, USA, 2018; ISBN 9788578110796.
2. Elsheikh, R.; Mohamed Shariff, A.R.B.; Amiri, F.; Ahmad, N.B.; Balasundram, S.K.; Soom, M.A.M. Agriculture Land Suitability Evaluator (ALSE): A decision and planning support tool for tropical and subtropical crops. *Comput. Electron. Agric.* **2013**, *93*, 98–110. [[CrossRef](#)]

3. Sanchez, P.A.; Palm, C.A.; Buol, S.W. Fertility capability soil classification: A tool to help assess soil quality in the Tropics. *Geoderma* **2003**, *114*, 157–185. [[CrossRef](#)]
4. Muyumba, D.K.; Liénard, A.; Mahy, G.; Luhembwe, M.N.; Colinet, G. Characterization of soil-plant systems in the hills of the Copper Belt in Katanga. A review. *Biotechnol. Agron. Soc. Environ.* **2015**, *19*, 204–214.
5. Ngongo, M.; Van Ranst, E.; Baert, G.; Kasongo, L.; Verdoodt, A.; Mujinya, B.B.; Mukalay, J. *Guide des sols en République Démocratique du Congo, Tome I: Étude et Gestion*; UGent, H.U., Ed.; Ecole Technique Salama-Don Bosco: Lubumbashi, Congo, 2009; ISBN 978-9-0767-6997-4.
6. Kasongo, L.M.E. Evaluation des terres à multiples Échelles pour la détermination de l' impact de la gestion agricole sur la sécurité alimentaire au Katanga, R.D. Congo. Ph.D. Thesis, Université de Gent, Gent, Belgium, 2008. Available online: <https://biblio.ugent.be/publication/607168/file/1883108> (accessed on 20 November 2025).
7. Alexandre, J. Les cuirasses lateritiques et autres formations ferrugineuses Tropicales exemple du Haut Katanga Méridional. *Mus. Roy. Afr. Centr. Tervuren. Ann. Sc. Géol.* **2002**, *107*, 129.
8. Tabu, I.; Lubobo, K.; Mbuya, K.; Kimuni, N. Heterosis and line-by-tester combining ability analysis for grain yield and provitamin a in maize. *SABRAO J. Breed. Genet.* **2023**, *55*, 695–707. [[CrossRef](#)]
9. Tabu, H.I.; Kankolongu, A.M.; Lubobo, A.K.; Kimuni, L.N. Maize yield and fall armyworm damage responses to genotype and sowing date-associated variations in weather conditions. *Eur. J. Agron.* **2024**, *161*, 127334. [[CrossRef](#)]
10. Ilunga, T.H.; Muganguz, N.T.; Kidinda, K.L.; Banza, M.J.; Nsenga, N.S.; Mpoyo, M.G.; Tshipama, T.D.; Lukusa, M.L.; Nyembo, K.L. Evaluation of maize response (*Zea mays* L.) to various modes and moments of chicken manure spreading in Lubumbashi, DR Congo. *Am. J. Plant Nutr. Fertil. Tech.* **2015**, *5*, 96–105. [[CrossRef](#)]
11. Nyembo, K.L.; Ilunga, T.H.; Mwamba, M.D.; Kanyenga, L.A.; Baboy, L.L.; Kalonji, M.A. *La Culture du Maïs Dans le Haut-Katanga; Etudes Africaines*; Harmattan: Paris, France, 2018; ISBN 978-2-343-14635-5.
12. Mujinya, B.B.; Adam, M.; Mees, F.; Bogaert, J.; Vranken, I.; Erens, H.; Baert, G.; Ngongo, M.; Van Ranst, E. Spatial patterns and morphology of termite (*Macrotermes falciger*) mounds in the Upper Katanga, D.R. Congo. *Catena* **2014**, *114*, 97–106. [[CrossRef](#)]
13. Adhikary, N.; Erens, H.; Weemaels, L.; Deweer, E.; Mees, F.; Mujinya, B.B.; Baert, G.; Boeckx, P.; Van Ranst, E. Effects of spreading out termite mound material on ferralsol fertility, Katanga, D.R. Congo. *Commun. Soil Sci. Plant Anal.* **2016**, *47*, 1089–1100. [[CrossRef](#)]
14. Nafi, E.; Webber, H.; Danso, I.; Naab, J.B.; Frei, M.; Gaiser, T. Interactive effects of conservation tillage, residue management, and nitrogen fertilizer application on soil properties under maize-cotton rotation system on highly weathered soils of West Africa. *Soil Tillage Res.* **2020**, *196*, 104473. [[CrossRef](#)]
15. Chen, C.; Singh, A.K.; Yang, B.; Wang, H.; Liu, W. Effect of termite mounds on soil microbial communities and microbial processes: Implications for soil carbon and nitrogen cycling. *Geoderma* **2023**, *431*, 116368. [[CrossRef](#)]
16. Santhoshkumar, S.; Gomathi, V.; Meenakshisundaram, P.; Kavitha Mary, J. Comparative insights of soil properties of termite hill in relation to the microbial community using culture-independent approach. *Tot. Environ. Adv.* **2024**, *9*, 200094. [[CrossRef](#)]
17. Apori, S.O.; Murongo, M.; Hanyabui, E.; Atiah, K.; Byalebeka, J. Potential of termite mounds and its surrounding soils as soil amendments in smallholder farms in Central Uganda. *BMC Res. Notes* **2020**, *13*, 397. [[CrossRef](#)]
18. Kpangba, T.P.M.K.; Mpika, J.; Makoundou, A.; Bita, M.A.; Attibayéba, A. Effect of the termite mounds on the vegetative production of three cultivars of black nightshade (*Solanum nigrum* L.: Solanaceae) grown in Brazzaville, Congo. *Int. J. Biol. Chem. Sci.* **2020**, *14*, 192–203. [[CrossRef](#)]
19. Jiao, F.; Hong, S.; Zhang, Q.; Li, M.; Shi, R.; Ma, Y.; Li, Q. Subsoiling before winter wheat cultivation increases photosynthetic characteristics and leaf water-use efficiency of summer maize in a double-cropping system. *Arch. Agron. Soil Sci.* **2023**, *69*, 847–860. [[CrossRef](#)]
20. Al-Irhayim, M.N.; Dahham, G.A.; Al-Mistawi, K.E.; Sedeeq, A.M. Determination of the force analysis of subsoiler plow tines using finite element method. *Curr. Appl. Sci. Technol.* **2025**, *25*, e0260201. [[CrossRef](#)]
21. Liu, X.; Liu, J.; Huang, C.; Liu, H.; Meng, Y.; Chen, H.; Ma, S.; Liu, Z. The impacts of irrigation methods and regimes on the water and nitrogen utilization efficiency in subsoiling wheat fields. *Agric. Water Manag.* **2024**, *295*, 108765. [[CrossRef](#)]
22. Jin, H.; Hongwen, L.; Xiaoyan, W.; McHugh, A.D.; Wenying, L.; Huanwen, G.; Kuhn, N.J. The adoption of annual subsoiling as conservation tillage in dryland maize and wheat cultivation in Northern China. *Soil Tillage Res.* **2007**, *94*, 493–502. [[CrossRef](#)]
23. Ning, T.; Liu, Z.; Hu, H.; Li, G.; Kuzyakov, Y. Physical, chemical and biological subsoiling for sustainable agriculture. *Soil Tillage Res.* **2022**, *223*, 105490. [[CrossRef](#)]
24. Ishaq, M.; Ibrahim, M.; Hassan, A.; Saeed, M.; Lal, R. Subsoil compaction effects on crops in Punjab, Pakistan: II. Root growth and nutrient uptake of wheat and sorghum. *Soil Tillage Res.* **2001**, *60*, 153–161. [[CrossRef](#)]
25. Singh, K.; Choudhary, O.P.; Singh, H.P.; Singh, A.; Mishra, S.K. Sub-soiling improves productivity and economic returns of cotton-wheat cropping system. *Soil Tillage Res.* **2019**, *189*, 131–139. [[CrossRef](#)]
26. Sun, Q.; Sun, W.; Zhao, Z.; Jiang, W.; Zhang, P.; Sun, X.; Xue, Q. Soil compaction and maize root distribution under subsoiling tillage in a wheat–maize double cropping system. *Agronomy* **2023**, *13*, 394. [[CrossRef](#)]

27. Cote, D.; Dupuis, G. Effets du sous-solage et du labour profond sur les propriétés physiques du sol et le rendement de la luzerne et du maïs sur loam sableux Chaloupe. *Can. J. Soil Sci.* **1980**, *60*, 345–353. [[CrossRef](#)]
28. Xie, G.; Liang, M.; Chen, P.; Zhang, C.; Fan, M.; Wang, C.; Zhao, L. The effects of tillage and the combined application of organic and inorganic fertilizers on the antioxidant enzyme activity and yield of maize leaves. *Agronomy* **2024**, *14*, 968. [[CrossRef](#)]
29. Wang, L.; Yu, X.; Gao, J.; Ma, D.; He, T.; Hu, S. Effect of subsoiling on the nutritional quality of grains of maize hybrids of different eras. *Plants* **2024**, *13*, 1900. [[CrossRef](#)]
30. Wei, X.; Guo, X.; Sparks, E.E.; Gao, W.; Ren, T.; Li, B.; Zhou, H. Conservation tillage increases maize (*Zea mays* L.) root lodging resistance through improving brace root development. *Soil Tillage Res.* **2025**, *254*, 106719. [[CrossRef](#)]
31. Lu, J.; Shao, H.; Jan Stomph, T.; Mi, G.; Yuan, L.; Evers, J. Maize root system phenotypes for efficient uptake of nitrogen and high yields. *Field Crops Res.* **2025**, *334*, 110154. [[CrossRef](#)]
32. Santos, T.E.D.; Gomes, F.H.; Mancini, M.; Nóbrega, G.N.; Avanzi, J.C.; Marques, J.J.; de Souza, V.S., Jr.; Inda, A.V.; Silva, M.L.N.; Curi, N. Detailed characterization of plinthic soils in Southern Mali, Sub-Saharan Africa, as a secure basis for specific soil management and food security. *Catena* **2023**, *226*, 107088. [[CrossRef](#)]
33. Mujinya, B.B.; Van Ranst, E.; Verdoodt, A.; Baert, G.; Ngongo, L.M. Termite bioturbation effects on electro-chemical properties of ferralsols in the Upper Katanga (D.R. Congo). *Geoderma* **2010**, *158*, 233–241. [[CrossRef](#)]
34. Ou, X.; Sebagenzi, G.D.; Mujinya, B.B.; Boeckx, P.; Döetler, S.; Six, J.; Shi, P.; Van Oost, K. From smallholder to commercial farming: The impact of termite mound levelling and spatial heterogeneity in mound morphology on soil organic carbon in Miombo Woodlands, Central Africa. *Landsc. Ecol.* **2025**, *40*, 83. [[CrossRef](#)]
35. Hamza, M.A.; Anderson, W.K. Soil compaction in cropping systems: A review of the nature, causes and possible solutions. *Soil Tillage Res.* **2005**, *82*, 121–145. [[CrossRef](#)]
36. Cai, H.; Ma, W.; Zhang, X.; Ping, J.; Yan, X.; Liu, J.; Yuan, J.; Wang, L.; Ren, J. Effect of subsoil tillage depth on nutrient accumulation, root distribution, and grain yield in spring maize. *Crop J.* **2014**, *2*, 297–307. [[CrossRef](#)]
37. Feng, X.; Hao, Y.; Latifmanesh, H.; Lal, R.; Cao, T.; Guo, J.; Deng, A.; Song, Z.; Zhang, W. Effects of subsoiling tillage on soil properties, maize root distribution, and grain yield on mollisols of Northeastern China. *Agron. J.* **2018**, *110*, 1607–1615. [[CrossRef](#)]
38. Asenso, E.; Hu, L.; Li, J.; Kai, T. Subsoiling improves soil physical properties and increases productivity in a maize farmland in Southern China. *Agric. Eng. Int.* **2022**, *2*, 23–34.
39. Jouquet, P.; Guilleux, N.; Ramesh, R. Influence of soil type on the properties of termite mound nests in Southern India. *Appl. Soil Ecol.* **2015**, *96*, 282–287. [[CrossRef](#)]
40. Jouquet, P.; Guilleux, N.; Caner, L.; Chintakunta, S.; Ameline, M.; Shanbhag, R.R. Influence of soil pedological properties on termite mound stability. *Geoderma* **2016**, *262*, 45–51. [[CrossRef](#)]
41. Jouquet, P.; Tessier, D.; Lepage, M. The soil structural stability of termite nests: Role of clays in *Macrotermes bellicosus* (Isoptera, Macrotermitinae) mound soils. *Eur. J. Soil Biol.* **2004**, *40*, 23–29. [[CrossRef](#)]
42. Abe, S.S.; Watanabe, Y.; Onishi, T.; Kotegawa, T.; Wakatsuki, T. Nutrient storage in termite (*Macrotermes bellicosus*) mounds and the implications for nutrient dynamics in a Tropical Savanna Ultisol. *Soil Sci. Plant Nutr.* **2011**, *57*, 786–795. [[CrossRef](#)]
43. Duponnois, R.; Paugy, M.; Thioulouse, J.; Masse, D.; Lepage, M. Functional diversity of soil microbial community, rock phosphate dissolution and growth of *Acacia seyal* as influenced by grass-, litter- and soil-feeding termite nest structure amendments. *Geoderma* **2005**, *124*, 349–361. [[CrossRef](#)]
44. Wang, L.; Guo, H.; Wang, L.; Cheng, D. Suitable tillage depth promotes maize yields by changing soil physical and chemical properties in a 3-year experiment in the North China Plain. *Sustainability* **2022**, *14*, 15134. [[CrossRef](#)]
45. Ji, B.; Zhao, Y.; Mu, X.; Liu, K.; Li, C. Effects of tillage on soil physical properties and root growth of maize in loam and clay in Central China. *Plant Soil Environ.* **2013**, *59*, 295–302. [[CrossRef](#)]
46. Sciarresi, C.; Thies, A.; Topp, C.; Eudy, D.; Trifunovic, S.; Ruiz, A.; Dixon, P.M.; Miguez, F.; Burras, L.C.; Archontoulis, S.V. Do newer maize hybrids grow roots faster and deeper? *Crop Sci.* **2024**, *64*, 1559–1576. [[CrossRef](#)]
47. King, A.E.; Ali, G.A.; Gillespie, A.W.; Wagner-Riddle, C. Soil organic matter as catalyst of crop resource capture. *Front. Environ. Sci.* **2020**, *8*, 50. [[CrossRef](#)]
48. World Reference Base for Soil Resources (WRB). *World Reference Base for Soil Resources. International Soil Classification System for Naming Soils and Creating Legends for Soil Maps*, 4th ed.; International Union of Soil Sciences (IUSS): Vienna, Austria, 2022; ISBN 9798986245119.
49. Assani, A.A. Analyse de la variabilité temporelle des précipitations (1916–1996) à Lubumbashi (Congo-Kinshasa) en relation avec certains indicateurs de la circulation atmosphériques (Oscillation Austral) et océaniques (El Niño/La Niña). *Sécheresse* **1999**, *10*, 245–252.
50. Malaisse, F. How to live and survive in Zambezian open forest (Miombo Ecoregion). *Les Pres. Agron. de Gembloux* **2011**, *23*, 91–97. [[CrossRef](#)]
51. Van Reeuwijk, L.P. *Procedures for Soil Analysis*, 6th ed.; International Soil Reference and Information Centre (ISRIC): Wageningen, The Netherlands, 2002.

52. Walkley, A.; Black, I.A. An examination of the Degtjareff method for determining soil organic matter, and a proposed modification of the chromic acid titration method. *Soil Sci.* **1934**, *37*, 29–38. [[CrossRef](#)]
53. Pribyl, D.W. A Critical review of the conventional SOC to SOM conversion factor. *Geoderma* **2010**, *156*, 75–83. [[CrossRef](#)]
54. Houba, J.; van Der Lee, J.; Novozamsky, I.; Walinga, I. *Soil and Plant Analysis: A Series of Syllabi: Part 5. Soil Analysis Procedures*; Department of Soil Science and Plant Nutrition, Agricultural University Wageningen: Wageningen, The Netherlands, 1988.
55. Tandzi, L.N.; Mutengwa, C.S. Estimation of maize (*Zea mays* L.) yield per harvest area: Appropriate methods. *Agronomy* **2020**, *10*, 29. [[CrossRef](#)]
56. Sapkota, T.B.; Jat, M.L.; Jat, R.K.; Kapoor, P.; Stirling, C. *Yield Estimation of Food and Non-Food Crops in Smallholder Production Systems*; Springer: Cham, Switzerland, 2016; ISBN 9783319297941.
57. Johnston, K.; Ver Hoef, J.M.; Krivoruchko, K.; Lucas, N. *Using ArcGis Geostatistical Analyst*, 1st ed.; ESRI Press: Redlands, CA, USA, 2001.
58. Smith, J.; Smith, P. *Environmental Modeling: An Introduction*; Oxford University Press: Oxford, UK, 2007; ISBN 9780199272068.
59. Harwell, M. A strategy for using Bias and RMSE as outcomes in Monte Carlo Studies in Statistics. *J. Mod. Appl. Stat. Methods* **2018**, *17*, 5. [[CrossRef](#)]
60. Hintze, J.L.; Nelson, R.D. Violin plots: A box plot-density trace synergism. *Am. Stat.* **1998**, *52*, 181–184. [[CrossRef](#)]
61. Shapiro, S.S.; Wilk, M.B. An analysis of variance test for normality (complete samples). *Biometrika* **1965**, *52*, 591–611. [[CrossRef](#)]
62. Tomczak, M.; Tomczak, E. The need to report effect size estimates revisited. an overview of some recommended measures of effect size. *Trends Sport Sci.* **2014**, *1*, 19–25.
63. Reimann, C.; Filzmoser, P.; Garrett, R.G.; Dutter, R. *Statistical data analysis explained: Applied environmental statistics with R*. In *Statistical Data Analysis Explained*; Wiley and Sons: Hoboken, NJ, USA, 2008; ISBN 978-0-470-98581-6.
64. Bedrick, E.J.; Tsai, C.-L. Model selection for multivariate regression in small samples. *Biometrics* **1994**, *50*, 226–231. [[CrossRef](#)]
65. Venables, W.N.; Ripley, B.D. *Modern Applied Statistics with S-Plus*, 4th ed.; Springer: New York, NY, USA, 2002.
66. Akinwande, M.O.; Dikko, H.G.; Samson, A. Variance inflation factor: As a condition for the inclusion of suppressor variable(s) in regression analysis. *Open J. Stat.* **2015**, *5*, 754–767. [[CrossRef](#)]
67. O'Brien, R.M. A Caution regarding rules of thumb for variance inflation factors. *Qual. Quant.* **2007**, *41*, 673–690. [[CrossRef](#)]
68. Burnham, K.P.; Anderson, D.R. Multimodel inference: Understanding AIC and BIC in model selection. *Sociol. Methods Res.* **2004**, *33*, 261–304. [[CrossRef](#)]
69. Nieminen, P. Application of standardized regression coefficient in meta-analysis. *BioMedInformatics* **2022**, *2*, 434–458. [[CrossRef](#)]
70. R Core Team. A language and environment for statistical computing. In *R Foundation for Statistical Computing*; R Core Team: Vienna, Austria, 2025.
71. Fritsch, E.; Herbillon, A.J.; Do Nascimento, N.R.; Grimaldi, M.; Melfi, A.J. From plinthic acrisols to plinthosols and gleysols: Iron and groundwater dynamics in the tertiary sediments of the Upper Amazon Basin. *Eur. J. Soil Sci.* **2007**, *58*, 989–1006. [[CrossRef](#)]
72. Rotta, L.R.; Paulino, H.B.; Anghinoni, I.; de Souza, E.D.; Lopes, G.; Carneiro, M.A.C. Phosphorus Fractions and Availability in a Haplic Plinthosol under No-Tillage System in the Brazilian Cerrado. *Ciência E Agrotecnologia* **2015**, *39*, 216–224. [[CrossRef](#)]
73. Asiamah, R.D.; Dwomo, O. Ethno-management of plinthic and ironpan soils in the Savanna Regions of West Africa. *Ghana J. Agric. Sci.* **2010**, *42*, 25–29. [[CrossRef](#)]
74. Laurent, J.Y.; Brossard, M. Etude comparee de la determination du phosphore total de sols Tropicaux. *Cah. ORSTOM Ser. Pedol.* **1991**, *26*, 281–285.
75. Gotz, L.F.; de Almeida, A.N.F.; de Souza Nunes, R.; Condron, L.M.; Pavinato, P.S. Assessment of phosphorus use and availability by contrasting crop plants in a Tropical Soil. *Biol. Fertil. Soils* **2024**, *60*, 603–612. [[CrossRef](#)]
76. Tshibangu Kazadi, A.; wa Lwalaba, J.L.; Kirika, A.B.; Mavungu, M.J.; Manda, K.G.; Iband, K.M.; Baert, G.; Haesaert, G.; Mukobo, M.R.P. Effect of phosphorus and Arbuscular Mycorrhizal Fungi (AMF) Inoculation on growth and productivity of Maize (*Zea mays* L.) in a Tropical Ferralsol. *Gesunde Pflanz* **2022**, *74*, 159–165. [[CrossRef](#)]
77. Mujinya, B.B.; Mees, F.; Erens, H.; Dumon, M.; Baert, G.; Boeckx, P.; Ngongo, M.; Van Ranst, E. Clay composition and properties in termite mounds of the Lubumbashi Area, D.R. Congo. *Geoderma* **2013**, *192*, 304–315. [[CrossRef](#)]
78. de Lima, S.S.; Pereira, M.G.; Pereira, R.N.; De Pontes, R.M.; Rossi, C.Q. Termite mounds effects on soil properties in the Atlantic Forest Biome. *Rev. Bras. Cienc. Solo* **2018**, *42*, 1011–1069. [[CrossRef](#)]
79. Padonou, E.A.; Djagoun, C.A.M.S.; Akakpo, A.B.; Ahlinvi, S.; Lykke, A.M.; Schmidt, M.; Assogbadjo, A.; Sinsin, B. Role of termites in the restoration of soils and plant richness on Bowé in West Africa. *Afr. J. Ecol.* **2020**, *58*, 828–835. [[CrossRef](#)]
80. Wang, X.; Geng, L.; Zhou, H.; Huang, Y.; Ji, J. Effects of subsoiling with different wing mounting heights on soil water infiltration using HYDRUS-2D Simulations. *Agronomy* **2023**, *13*, 2742. [[CrossRef](#)]
81. Huang, C.; Liu, X.; Gao, Y.; Chen, H.; Ma, S.; Qin, A.; Zhang, Y.; Gao, Z.; Song, Y.; Sun, J.; et al. Response of *Triticum vulgare* growth and nitrogen allocation to irrigation methods and regimes under subsoiling tillage. *Agronomy* **2024**, *14*, 858. [[CrossRef](#)]
82. Šarauski, E.; Sokas, S.; Rukaitė, J. Variable depth tillage: Importance, applicability, and impact—An overview. *AgriEngineering* **2024**, *6*, 1870–1885. [[CrossRef](#)]

83. Alonso, M.; López, G.; Grajales, M. Mejoramiento de las propiedades hidráulicas del suelo en el cultivo de soya mediante el subsuelo. *Rev. Mex. De Cienc. Agric.* **2023**, *14*, 78–89.
84. Erens, H.; Mujinya, B.B.; Mees, F.; Baert, G.; Boeckx, P.; Malaisse, F.; Van Ranst, E. The origin and implications of variations in soil-related properties within *Macrotermes falciger* mounds. *Geoderma* **2015**, *249–250*, 40–50. [[CrossRef](#)]
85. Mehlich, A. Mehlich 3 soil test extractant: A modification of Mehlich 2 extractant. *Commun Soil Sci. Plant Anal.* **1984**, *15*, 1409–1416. [[CrossRef](#)]
86. Olsen, S.R.; Cole, C.V.; Watanabe, F.S.; Dean, L.A. *Estimation of Available Phosphorus in Soils by Extraction with Sodium Bicarbonate*; US Government Printing Office: Washington, DC, USA, 1954.
87. Garba, M.; Cornelis, W.M.; Steppe, K. Effect of termite mound material on the physical properties of sandy soil and on the growth characteristics of tomato (*Solanum lycopersicum* L.) in Semi-Arid Niger. *Plant Soil* **2011**, *338*, 451–466. [[CrossRef](#)]
88. Tilahun, A.; Cornelis, W.; Sleutel, S.; Nigussie, A.; Dume, B.; Van Ranst, E. The potential of termite mound spreading for soil fertility management under low input subsistence agriculture. *Agriculture* **2021**, *11*, 1002. [[CrossRef](#)]
89. Sajid, A.; Ahmad, K.; Khan, Z.I.; Khalofah, A.; Ahmad, I. Assessing the impact of industrial pollution stress on the physiological defense, proximate composition and morphological traits of riparian vegetation. *BMC Plant Biol.* **2025**, *25*, 992. [[CrossRef](#)] [[PubMed](#)]
90. Luo, M.; Vandeputte, D.J.; Lievens, S.; Li, G.; Su, Y.; Huysmans, M.; Elskens, M.; Baeyens, W.; Gao, Y. Understanding the availability of metals in agricultural soils and the impact of manure application. *J. Hazard. Mater.* **2025**, *493*, 138386. [[CrossRef](#)] [[PubMed](#)]
91. Wala, M.; Kołodziejek, J.; Sieczyńska, K.; Mazur, J.; Skwarek-Fadecka, M. Manganese and iron toxicity in invasive tree tobacco (*Nicotiana glauca* Graham, Solanaceae). *South Afr. J. Bot.* **2025**, *186*, 486–496. [[CrossRef](#)]
92. Bell, L.E.; Moir, J.L.; Black, A.D. The effects of soil acidity and aluminium on the root systems and shoot growth of *Lotus pedunculatus* and *Lupinus polyphyllus*. *Plants* **2024**, *13*, 2268. [[CrossRef](#)] [[PubMed](#)]
93. Li, K.; Lu, H.; Nkoh, J.N.; Hong, Z.; Xu, R. Aluminum mobilization as influenced by soil organic matter during soil and mineral acidification: A constant pH study. *Geoderma* **2022**, *418*, 115853. [[CrossRef](#)]
94. Jansen, B.; Nierop, K.G.J.; Verstraten, J.M. Mechanisms controlling the mobility of dissolved organic matter, aluminium and iron in Podzol B horizons. *Eur. J. Soil Sci.* **2005**, *56*, 537–550. [[CrossRef](#)]
95. Hernandez-Soriano, M.C.; Jimenez-Lopez, J.C. Effects of soil water content and organic matter addition on the speciation and bioavailability of heavy metals. *Scie. Tot. Environ.* **2012**, *423*, 55–61. [[CrossRef](#)]
96. Chisanga, K.; Mbega, E.R.; Ndakidemi, P.A. Prospects of using termite mound soil organic amendment for enhancing soil nutrition in Southern Africa. *Plants* **2020**, *9*, 649. [[CrossRef](#)] [[PubMed](#)]
97. Brauman, A. Effect of gut transit and mound deposit on soil organic matter transformations in the soil feeding termite: A review. *Eur. J. Soil Biol.* **2000**, *36*, 117–125. [[CrossRef](#)]
98. Berggren, D.; Mulder, J. The role of organic matter in controlling aluminum solubility in acidic mineral soil horizons. *Geochim. Cosmochim. Acta* **1995**, *59*, 4167–4180. [[CrossRef](#)]
99. Tabu, H.I.; Tshiabukole, J.P.K.; Kankolongo, A.M.; Lubobo, A.K.; Kimuni, L.N. Yield stability and agronomic performances of provitamin A maize (*Zea mays* L.) genotypes in South-East of DR Congo. *Open Agric.* **2023**, *8*, 120220177. [[CrossRef](#)]
100. Ilunga, T.H.; Banza, M.J.; Lukusa, M.L.; Mukunto, K.I.; Malonga, H.L.; Kanyenga, L.A.; Nyembo, K.L. Influence du moment d’application du NPK sur la croissance et le rendement du maïs (*Zea mays* L.) installé sur un ferralsol. *J. Appl. Biosci.* **2019**, *127*, 12794. [[CrossRef](#)]
101. Kimuni Luciens, N.; Sikuzani Yannick, U.; Mubemba Michel, M.; Mugisho David, B.; Lenge Emery, K.; Longanza Louis, B. Effets des apports des doses variées de fertilisants inorganiques (NPKS et Urée) sur le rendement et la rentabilité économique de nouvelles variétés de *Zea mays* L. à Lubumbashi, Sud-Est de La RD Congo. *J. Appl. Biosci.* **2012**, *59*, 4286–4296.
102. Banza, M.J.; Mwamba, K.F.; Esoma, E.B.; Meta, T.M.; Mayamba, M.G.; Kasongo, L.M.E. Evaluation de la réponse du maïs (*Zea mays* L.) installé entre les haies de tithonia diversifolia à Lubumbashi, R.D. Congo. *J. Appl. Biosci.* **2019**, *134*, 13643. [[CrossRef](#)]
103. Zhou, P.; Wang, S.; Guo, L.; Shen, Y.; Han, H.; Ning, T.; Paper, O. Effects of subsoiling stage on summer maize water use efficiency and yield in North China Plains. *Plant Soil Environ.* **2019**, *65*, 556–562. [[CrossRef](#)]
104. Chen, G.; Weil, R.R. Root Growth and Yield of Maize as Affected by Soil Compaction and Cover Crops. *Soil Tillage Res.* **2011**, *117*, 17–27. [[CrossRef](#)]
105. Wang, Y.; Chen, Y.; Rahman, S.; Froese, J. Tillage effects on soil penetration resistance and early crop growth for red river clay. *Can. Biosyst. Eng.* **2009**, *51*, 11.
106. Grevers, M.C.J.; De Jong, E. Soil structure and crop yield over a s-year period following subsoiling solonchic and chernozemic soils in Saskatchewan. *Can. J. Soil Sci.* **1993**, *91*, 81–91. [[CrossRef](#)]
107. Ramadhan, M.N.; Alfaris, M.A.A. Soil properties and maize growth as affected by subsoiling and traffic-induced compaction. *IOP Conf. Ser. Earth Environ. Sci.* **2023**, *1225*, 012077. [[CrossRef](#)]
108. Li, X.; Wang, R.; Lou, F.; Ji, P.; Wang, J.; Dong, W.; Tao, P.; Zhang, Y. Subsoiling combine with layered nitrogen application optimizes root distribution and improve grain yield and n efficiency of summer maize. *Agronomy* **2024**, *14*, 1228. [[CrossRef](#)]

109. Wu, J.; Wang, R.; Zhao, W.; Zhao, K.; Wu, S.; Zhang, J.; Wang, H.; Fu, G.; Huang, M.; Li, Y. Combined subsoiling and ridge-furrow rainfall harvesting during the summer fallow season improves wheat yield, water and nutrient use efficiency, and quality and reduces soil nitrate-n residue in the dryland summer fallow-winter wheat rotation. *Front Plant Sci.* **2024**, *15*, 1401287. [[CrossRef](#)] [[PubMed](#)]
110. Sikuzani, Y.U.; Ilunga, G.M.; Mulembo, T.M.; Katombe, B.N.; Wa Lwalaba, J.L.; Lukangila, M.A.; Lubobo, A.K.; Longanza, L.B. Amélioration de la qualité des sols acides de Lubumbashi (Katanga, RD Congo) par l'application de différents niveaux de compost de fumiers de poules. *J. Appl. Biosci.* **2014**, *77*, 6523–6533. [[CrossRef](#)]
111. Boansi, D.; Owusu, V.; Donkor, E. Impact of integrated soil fertility management on maize yield, yield gap and income in Northern Ghana. *Sustain. Futures* **2024**, *7*, 100185. [[CrossRef](#)]
112. Nikkel, M.; Lima, S.O. Maize (*Zea mays*) cultivated in concretionary petric plinthosol. *J. Agric. Sci.* **2019**, *11*, 131. [[CrossRef](#)]
113. Jouquet, P.; Mamou, L.; Lepage, M.; Velde, B. Effect of termites on clay minerals in Tropical soils: Fungus-Growing termites as weathering agents. *Eur. J. Soil Sci.* **2002**, *53*, 521–528. [[CrossRef](#)]
114. Suleymanov, A.; Nizamutdinov, T.; Morgun, E.; Abakumov, E. Evaluation and spatial variability of cryogenic soil properties (Yamal-Nenets Autonomous District, Russia). *Soil Syst.* **2022**, *6*, 65. [[CrossRef](#)]
115. Zingore, S.; Murwira, H.K.; Delve, R.J.; Giller, K.E. Influence of nutrient management strategies on variability of soil fertility, crop yields and nutrient balances on smallholder farms in Zimbabwe. *Agric. Ecosyst. Environ.* **2007**, *119*, 112–126. [[CrossRef](#)]
116. Stoyanova, Z.; Poschenrieder, C.; Tzvetkova, N.; Doncheva, S. Characterization of the tolerance to excess manganese in four maize varieties. *Soil Sci. Plant Nutr.* **2009**, *55*, 747–753. [[CrossRef](#)]
117. Karlsson, T.; Persson, P.; Skyllberg, U. Complexation of Copper (II) in organic soils and in dissolved organic matter-EXAFS Evidence for Chelate Ring Structures. *Environ. Sci. Technol.* **2006**, *40*, 2623–2628. [[CrossRef](#)] [[PubMed](#)]
118. Yin, Y.; Impellitteri, C.A.; You, S.-J.; Allen, H.E. The Importance of Organic Matter Distribution and Extract Soil: Solution Ratio on the Desorption of Heavy Metals from Soils. *Sci. Total Environ.* **2002**, *287*, 107–119. [[CrossRef](#)] [[PubMed](#)]
119. Sanders, J.R. The effect of pH upon the copper and cupric ion concentrations in soil solutions. *Eur. J. Soil Sci.* **2006**, *4*, 679–689. [[CrossRef](#)]
120. Yruela, I. Copper in Plants: Acquisition, transport and interactions. *Funct. Plant Biol.* **2009**, *36*, 409–430. [[CrossRef](#)]
121. Stoyanova, Z.; Zozikova, E.; Poschenrieder, C.; Barcelo, J.; Doncheva, S. The effect of silicon on the symptoms of manganese toxicity in maize plants. *Acta Biol. Hung.* **2008**, *59*, 479–487. [[CrossRef](#)]
122. da Silva, A.P.V.; Silva, A.O.; de Lima, F.R.D.; Benedet, L.; Carriço, C.O.; Franco, A.d.J.; Guilherme, L.R.G.; Carneiro, M.A.C. Reduction of pH on the bioavailability of potentially toxic elements for plants grown in iron mining tailing. *Water Air Soil Pollut.* **2024**, *235*, 409. [[CrossRef](#)]
123. Hou, S.; Zheng, N.; Tang, L.; Ji, X.; Li, Y. Effect of soil pH and organic matter content on heavy metals availability in maize (*Zea mays* L.) rhizospheric soil of non-ferrous metals smelting area. *Environ. Monit. Assess* **2019**, *191*, 634. [[CrossRef](#)]
124. Li, J.; Xu, Y.; Zhang, Y.; Liu, Z.; Gong, H.; Fang, W.; Ouyang, Z.; Li, W.; Xu, L. Quantifying the mitigating effect of organic matter on heavy metal availability in soils with different manure applications: A geochemical modelling study. *Ecotoxicol. Environ. Saf.* **2024**, *276*, 116321. [[CrossRef](#)]
125. Montiel-Rozas, M.M.; Madejón, E.; Madejón, P. Effect of heavy metals and organic matter on root exudates (Low Molecular Weight Organic Acids) of herbaceous species: An assessment in sand and soil conditions under different levels of contamination. *Environ. Poll.* **2016**, *216*, 273–281. [[CrossRef](#)]
126. Ngon Ngon, G.F.; Yongue-Fouateu, R.; Bitom, D.L.; Bilong, P. A Geological study of clayey laterite and clayey hydromorphic material of the region of Yaoundé (Cameroon): A prerequisite for local material promotion. *J. Afr. Earth Sci.* **2009**, *55*, 69–78. [[CrossRef](#)]
127. Soil Survey Staff. *Keys to Soil Taxonomy*, 12th ed.; USDA-NRCS: Washington, DC, USA, 2014; Volume 12, ISBN 0926487221.
128. Foy, C.D.; Chaney, R.L.; White, M.C. The physiology of metal toxicity in plants. *Ann. Rev. Plant Phys.* **1978**, *29*, 511–566. [[CrossRef](#)]
129. Ryder, M.; Gérard, F.; Evans, D.E.; Hodson, M.J. The use of root growth and modelling data to investigate amelioration of aluminium toxicity by silicon in picea abies seedlings. *J. Inorg. Biochem.* **2003**, *97*, 52–58. [[CrossRef](#)] [[PubMed](#)]
130. Lidon, F.C.; Barreiro, M.G. Threshold aluminum toxicity in maize. *J. Plant Nutr.* **1998**, *21*, 413–419. [[CrossRef](#)]
131. Doncheva, S.; Poschenrieder, C.; Stoyanova, Z.; Georgieva, K.; Velichkova, M.; Barceló, J. Silicon amelioration of manganese toxicity in mn-sensitive and mn-tolerant maize varieties. *Environ. Exp. Bot.* **2009**, *65*, 189–197. [[CrossRef](#)]
132. Fageria, N.K. Adequate and toxic levels of copper and manganese in upland rice, common bean, corn, soybean, and wheat grown on an oxisol. *Commun. Soil Sci. Plant Anal.* **2001**, *32*, 1659–1676. [[CrossRef](#)]
133. Khoshru, B.; Mitra, D.; Nosratabad, A.F.; Reyhanitabar, A.; Mandal, L.; Farda, B.; Djebaili, R.; Pellegrini, M.; Guerra-Sierra, B.E.; Senapati, A.; et al. Enhancing manganese availability for plants through microbial potential: A sustainable approach for improving soil health and food security. *Bacteria* **2023**, *2*, 129–141. [[CrossRef](#)]
134. Mundus, S.; Lombi, E.; Holm, P.E.; Zhang, H.; Husted, S. Assessing the plant availability of manganese in soils using diffusive gradients in thin films (DGT). *Geoderma* **2012**, *183–184*, 92–99. [[CrossRef](#)]

135. Moriasi, D.N.; Arnold, J.G.; Van Liew, M.W.; Bingner, R.L.; Harmel, R.D.; Veith, T.L. Model evaluation guidelines for systematic quantification of accuracy in watershed simulations. *Trans. ASABE* **2007**, *50*, 885–900. [[CrossRef](#)]
136. Olaluwoye, O.T.; Lukman, A.F.; Alrasheedi, M.A.; Nzomo, W.N.; Farghali, R.A. Robust Estimation Methods for Addressing Multicollinearity and Outliers in Beta Regression Models. *Sci. Rep.* **2025**, *15*, 11649. [[CrossRef](#)]
137. O'Brien, F.J.M.; Almaraz, M.; Foster, M.A.; Hill, A.F.; Huber, D.P.; King, E.K.; Langford, H.; Lowe, M.A.; Mickan, B.S.; Miller, V.S.; et al. Soil Salinity and pH Drive Soil Bacterial Community Composition and Diversity along a Lateritic Slope in the Avon River Critical Zone Observatory, Western Australia. *Front. Microbiol.* **2019**, *10*, 1486. [[CrossRef](#)]
138. Huang, S.; Islam, M.U.; Jiang, F. The Effect of Deep-Tillage Depths on Crop Yield: A Global Meta-Analysis. *Plant Soil Environ.* **2023**, *69*, 105–117. [[CrossRef](#)]
139. Yang, P.; Dong, W.; Heinen, M.; Qin, W.; Oenema, O. Soil Compaction Prevention, Amelioration and Alleviation Measures Are Effective in Mechanized and Smallholder Agriculture: A Meta-Analysis. *Land* **2022**, *11*, 645. [[CrossRef](#)]
140. Jee, H.K.; Park, J.H. Mitigating manganese phytoavailability in Cr(III)-Contaminated soils using biochar and lime. *Environ. Poll. Bioavail.* **2025**, *37*, 2543318. [[CrossRef](#)]
141. Shafique, F.; Ali, Q.; Yasin, G.; Ahmad, S.; Shafeeq, T.; Zaheer, A.; Malik, A. Heavy metal toxicity and its physio-biochemical effects on maize. *Plant Cell Biotechnol. Mol. Biol.* **2020**, *21*, 94–102.
142. Michener, W.K. Quantitatively evaluating restoration experiments: Research design, statistical analysis, and data management considerations. *Restor. Ecol.* **1997**, *5*, 324–337. [[CrossRef](#)]
143. Hayward, M.W.; Boitani, L.; Burrows, N.D.; Funston, P.J.; Karanth, K.U.; Mackenzie, D.I.; Pollock, K.H.; Yarnell, R.W. Ecologists need robust survey designs, sampling and analytical methods. *J. Appl. Ecol.* **2015**, *52*, 286–290. [[CrossRef](#)]

**Disclaimer/Publisher's Note:** The statements, opinions and data contained in all publications are solely those of the individual author(s) and contributor(s) and not of MDPI and/or the editor(s). MDPI and/or the editor(s) disclaim responsibility for any injury to people or property resulting from any ideas, methods, instructions or products referred to in the content.